DNA damage response activates respiration and thereby enlarges dNTP pools to promote cell survival in budding yeast

Received for publication, December 20, 2018, and in revised form, April 30, 2019 Published, Papers in Press, May 9, 2019, DOI 10.1074/jbc.RA118.007266

Pengli Bu[‡], Shreya Nagar[‡], Madhura Bhagwat[‡], Pritpal Kaur[‡], Ankita Shah[§1], Joey Zeng[‡2], Ivana Vancurova[‡], and Ales Vancura[‡3]

From the Departments of [‡]Biological Sciences and [§]Pharmaceutical Sciences, St. John's University, Queens, New York 11439

Edited by George M. Carman

The DNA damage response (DDR) is an evolutionarily conserved process essential for cell survival. Previously, we found that decreased histone expression induces mitochondrial respiration, raising the question whether the DDR also stimulates respiration. Here, using oxygen consumption and ATP assays, RT-qPCR and ChIP-qPCR methods, and dNTP analyses, we show that DDR activation in the budding yeast *Saccharomyces cerevisiae*, either by genetic manipulation or by growth in the presence of genotoxic chemicals, induces respiration. We observed that this induction is conferred by reduced transcription of histone genes and globally decreased DNA nucleosome occupancy. This globally altered chromatin structure increased the expression of genes encoding enzymes of tricarboxylic acid cycle, electron transport chain, oxidative phosphorylation, elevated oxygen consumption, and ATP synthesis. The elevated ATP levels resulting from DDR-stimulated respiration drove enlargement of dNTP pools; cells with a defect in respiration failed to increase dNTP synthesis and exhibited reduced fitness in the presence of DNA damage. Together, our results reveal an unexpected connection between respiration and the DDR and indicate that the benefit of increased dNTP synthesis in the face of DNA damage outweighs possible cellular damage due to increased oxygen metabolism.

All cells face constant challenge to protect their genome integrity. Insults that can directly or indirectly damage DNA arise from inside as well as outside the cell, including normal metabolic processes, DNA replication, UV light and ionizing radiation, and chemical exposure (1–3). Because maintenance of genome stability is crucial for survival, cells have evolved a set of highly-conserved mechanisms to sense and repair damaged DNA, which are collectively referred to as the DNA damage response (DDR)[4] (4, 5). A cascade of protein kinases known as the "checkpoint kinases" is the key component of the DDR (Fig. 1 and Table 1) (6–9). In the presence of damaged DNA, the sensor kinases (ATM/ATR in mammals and Tel1/Mec1 in budding yeast) become active and phosphorylate the effector kinases (CHK1 and CHK2 in mammals and Chk1p and Rad53p in budding yeast) (10). Rad53p, the yeast ortholog of CHK2, is an essential intermediate kinase in the checkpoint pathway, as it connects the upstream kinases and downstream effectors to mediate an array of cellular outcomes in response to DNA damage (6, 11, 12). One of the Rad53p targets is another checkpoint kinase Dun1p (13).

Activation of the checkpoint kinases results in cell cycle arrest, activation of DNA repair, and reprogramming of transcription. One of the key outcomes of the DDR in yeast is the enlargement of the deoxyribonucleoside triphosphate (dNTP) pools, which is a prerequisite for effective DNA repair (Fig. 1) (14, 15). The rate-limiting step of dNTP synthesis is the reduction of ribonucleoside diphosphates into corresponding deoxyribonucleoside diphosphates, catalyzed by ribonucleotide reductase (RNR) (16). In most eukaryotes, RNR enzymes are $\alpha 2\beta 2$ heterotetramers, in which the $\alpha 2$ homodimer and the $\beta 2$ homodimer represent the large and small subunits, respectively. In yeast, however, the small subunit is a heterodimer of Rnr2p and Rnr4p; the large subunit is a homodimer of Rnr1p. The catalytic site is contained within the large subunit of both mammalian and yeast RNR enzymes. Both mammalian and yeast RNR genes are regulated transcriptionally, and the enzymes are regulated allosterically (17–19). In yeast, transcription of *RNR2*, *RNR3*, and *RNR4* genes is induced following checkpoint activation and Dun1p-mediated phosphorylation and inactivation of the transcriptional repressor Crt1p (20). Transcription of *RNR1* is regulated in a cell cycle–dependent manner by the transcriptional complex MBF and by high mobility group-domain protein Ixr1p, but not by Crt1p (21–24). Dun1p regulates RNR activity and dNTP synthesis by at least two additional mechanisms. Dun1p phosphorylates Dif1p, a protein required for nuclear localization of Rnr2p and Rnr4p. Phosphorylation of Dif1p by Dun1p releases Rnr2p and Rnr4p

This work was supported by National Institutes of Health Grant GM120710 (to A. V). The authors declare that they have no conflicts of interest with the contents of this article. The content is solely the responsibility of the authors and does not necessarily represent the official views of the National Institutes of Health.

[1] Present address: Freund-Vector Corp., 675 44th St., Marion, IA 52302.

[2] Present address: Harvard School of Dental Medicine, 188 Longwood Ave., Boston, MA 02115.

[3] To whom correspondence should be addressed: Dept. of Biological Sciences, St. John's University, 8000 Utopia Pkwy., Queens, NY 11439. Tel.: 718-990-1679; Fax: 718-990-5958; E-mail: vancuraa@stjohns.edu.

[4] The abbreviations used are: DDR, DNA damage response; ATM, ataxia telangiectasia–mutated; ATR, ATM and Rad3-related protein; ChIP, chromatin immunoprecipitation coupled with quantitative PCR; ETC, electron transport chain; 4-NQO, 4-nitroquinoline 1-oxide; OXPHOS, oxidative phosphorylation; RNR, ribonucleotide reductase; ROS, reactive oxygen species; RT-qPCR, real-time reverse transcription quantitative PCR; YPD, yeast extract/peptone/dextrose; TCA, tricarboxylic acid; MMS, methylmethane sulfonate; pol, polymerase.

Table 1
Genes/proteins used in this study

Gene	Function
ASF1	Nucleosome assembly factor and histone chaperone
CHK1	Effector kinase in DNA damage checkpoint
CIT1	Citrate synthase, the first enzyme of the TCA cycle
COX1	Subunit of cytochrome *c* oxidase, enzyme of the ETC
CRT1	Transcriptional repressor of DNA damage–regulated genes
CYC1	Cytochrome *c* (isoform 1); component of the ETC
CYT1	Cytochrome c_1, component of the ETC
DUN1	Protein kinase involved in DDR; functions downstream of Rad53
HAP1	Transcription factor regulated by heme; regulates expression of respiratory genes
HAP4	Subunit of the Hap2/3/4/5 transcription complex; regulator of respiratory genes
HIR1	Subunit of the HIR complex; involved in regulation of histone gene transcription
HHF1	Histone H4; one of two identical histone H4 proteins
HHF2	Histone H4; one of two identical histone H4 proteins
HHT1	Histone H3; one of two identical histone H3 proteins
HHT2	Histone H3; one of two identical histone H3 proteins
HTA1	Histone H2A; one of two nearly identical H2A proteins
HTA2	Histone H2A; one of two nearly identical H2A proteins
HTB1	Histone H2B; one of two nearly identical H2B proteins
HTB2	Histone H2B; one of two nearly identical H2B proteins
IDH1	Subunit of isocitrate dehydrogenase; enzyme of the TCA cycle
MBP1	Transcription factor; with Swi6 forms MBF complex
MEC1	Sensor kinase in DNA damage checkpoint; yeast ortholog of ATR
QCR7	Subunit of ubiquinol cytochrome *c* reductase; component of the ETC
RAD52	Required for DNA double-strand break repair and homologous recombination
RAD53	Effector kinase in DNA damage checkpoint; functions downstream of Mec1
RNR1	Major isoform of large subunit of the RNR complex
RNR2	Small subunit of the RNR complex
RNR3	Minor isoform of large subunit of the RNR complex
RNR4	Small subunit of the RNR complex
SML1	Inhibitor of the RNR complex
SWI6	Transcription factor; subunit of SBF and MBF complexes
TEL1	Sensor kinase in DNA damage checkpoint; yeast ortholog of ATM
TOM1	E3 ubiquitin ligase involved in degradation of excess histones

into the cytoplasm, where they assemble with Rnr1p to form an active RNR enzyme (25–30). During S phase or after DNA damage, Dun1p also phosphorylates and induces degradation of Sml1p, a protein that binds and inhibits the Rnr1p subunit (Fig. 1) (31–34).

Proliferating cells need to maintain a delicate balance between histone and DNA synthesis to ensure correct stoichiometric amounts for chromatin assembly and to avoid genome instability (35, 36). Treatment with genotoxic agents that damage DNA or interfere with DNA replication triggers repression of histone genes (37–39). We have previously shown that a decrease in histone expression induces respiration (40). This poses an intriguing question: does DDR induce mitochondrial respiration? One of the sources of reactive oxygen species (ROS) is the oxidative electron transport chain (ETC) in the mitochondria. It is widely believed that DDR results in down-regulation of respiration to protect DNA from endogenous ROS (41–43). Surprisingly, our data show that DDR and growth in the presence of sublethal concentrations of genotoxic chemicals activate respiration to increase ATP production and to elevate dNTP levels, which are required for efficient DNA repair and cell survival upon DNA damage.

Results

DDR stimulates aerobic respiration

To determine whether DDR stimulates respiration, we used two approaches to introduce DDR. The first approach utilized

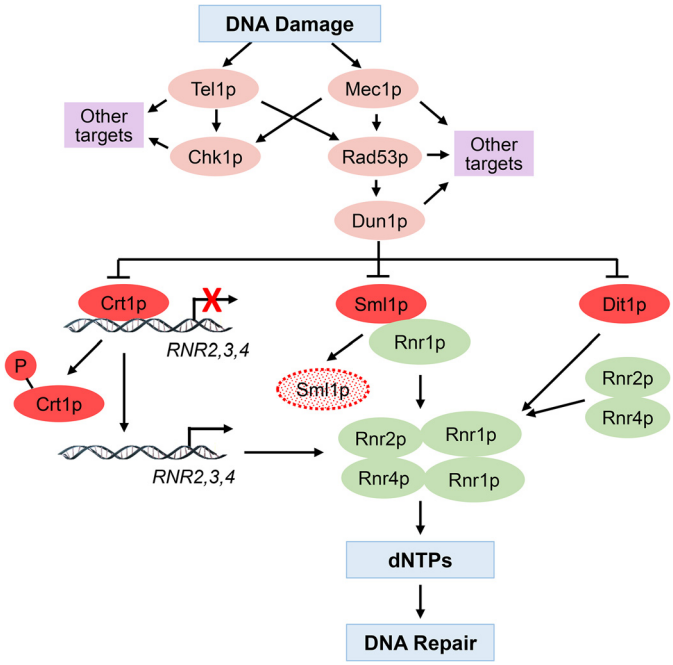

Figure 1. Model depicting the role of checkpoint kinases in DDR, RNR regulation, and synthesis of dNTPs. DNA damage activates the cascade of checkpoint kinases Mec1p, Rad53p, and Dun1p. Dun1p phosphorylates and down-regulates three negative regulators of the RNR complex: Crt1p, Sml1p, and Dif1p. Crt1p is a transcriptional repressor recruited to the *RNR2*, *RNR3*, and *RNR4* genes. Phosphorylation of Crt1p derepresses *RNR2*, *RNR3*, and *RNR4* genes by inducing dissociation of Crt1p from the corresponding promoters. Sml1p binds Rnr1p and inhibits RNR activity. Sml1p phosphorylation promotes its ubiquitylation and degradation by the 26S proteasome. Dif1p regulates nucleocytosolic distribution of Rnr2p and Rnr4p. Dun1p-mediated phosphorylation of Dif1p leads to redistribution of Rnr2p and Rnr4p from the nucleus to the cytoplasm, where Rnr1p resides, resulting in assembly of the active RNR complex. The cumulative effect of Dun1p activation is increased RNR assembly and activity and increased synthesis of dNTPs.

the genotoxic chemicals bleocin and 4-nitroquinoline 1-oxide (4-NQO). Bleocin belongs to the antibiotic bleomycin family and causes DNA double-strand breaks (44). 4-NQO mimics the effect of UV light and forms DNA adducts (45). Both bleocin and 4-NQO trigger DDR. When compared with control cells, cells grown in the presence of sublethal concentrations of either chemical consumed more oxygen and produced more ATP, two parameters reflecting the activity of aerobic respiration in the mitochondria (Fig. 2, *A* and *B*) (40, 46). Oxygen consumption of cells treated with bleocin or 4-NQO increased 1.8- and 1.5-fold, respectively, whereas the cellular ATP level increased 2.6- and 2.0-fold, respectively (Fig. 2, *A* and *B*).

The second approach to introduce DDR employed *rad52*Δ mutation. *RAD52* is required for DNA double-strand break repair and homologous recombination. Inactivation of *RAD52* renders cells unable to repair DNA strand breaks and thereby triggers DDR (47). Compared with WT cells, *rad52*Δ cells consumed 1.6 times more oxygen and displayed 3.2 times increased ATP levels (Fig. 2*C*).

Checkpoint kinases Mec1p and Rad53p are required for DDR-induced respiration

DDR is mediated through activation of checkpoint kinases and their cellular targets, which coordinate cell cycle arrest and repair of damaged DNA (Fig. 1). To investigate the requirement

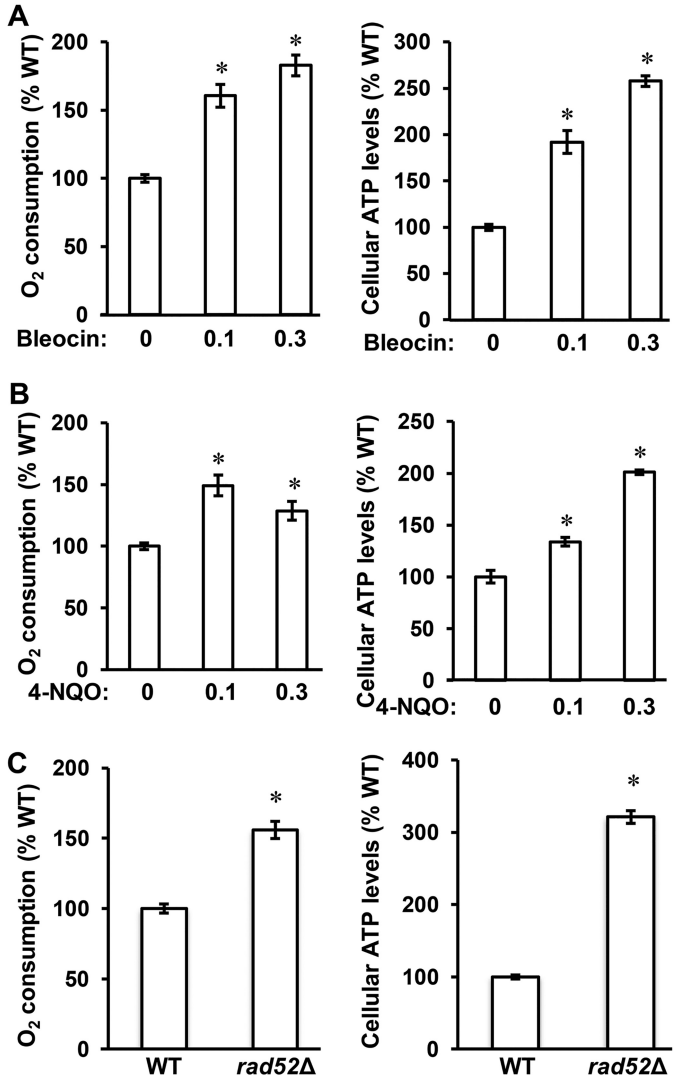

Figure 2. DDR stimulates respiration. *A* and *B*, cellular oxygen consumption rate and ATP levels in WT cells (WT, W303-1a) grown in YPD medium in the presence of bleocin at 0, 0.1 and 0.3 μg/ml (*A*) and 4-NQO at 0, 0.1 and 0.3 μg/ml (*B*). *C*, cellular oxygen consumption rate and ATP levels in WT and *rad52*Δ cells. The experiments were repeated three times, and the results are shown as means ± S.D. Values that are statistically significantly different ($p < 0.05$) from the WT cells are indicated by an *asterisk*. The results are expressed relative to the value for the WT strain.

of the checkpoint kinases Mec1p, Tel1p, Chk1p, Rad53p, and Dun1p for induction of respiration, we introduced the corresponding mutations into *rad52*Δ cells and determined oxygen consumption (Fig. 3*A*). The oxygen consumption of *tel1*Δ cells was elevated compared with WT cells, and introducing the *tel1*Δ mutation into the *rad52*Δ cells further increased oxygen consumption above the *rad52*Δ level. *chk1*Δ cells consumed less oxygen than WT cells, and the oxygen consumption of the *rad52*Δ*chk1*Δ cells was attenuated compared with *rad52*Δ cells. Because *mec1*Δ and *rad53*Δ cells are viable only if harboring *crt1*Δ or *sml1*Δ mutations (20, 31), we measured oxygen consumption in *mec1*Δ*sml1*Δ, *mec1*Δ*crt1*Δ, *rad53*Δ*sml1*Δ, and *rad53*Δ*crt1*Δ strains. Surprisingly, *mec1*Δ*sml1*Δ and *rad53*Δ*sml1*Δ strains displayed increased oxygen consumption compared with WT cells. This increase can be attributed to the *sml1*Δ mutation, because *sml1*Δ cells also displayed slightly increased oxygen consumption. This finding is not entirely surprising, because *sml1*Δ cells display increased copy number of mitochondrial DNA, likely due to the elevated dNTP level (48). The oxygen consumption in *rad53*Δ*crt11*Δ was comparable with WT cells, while the oxygen consumption of *mec1*Δ*crt1*Δ cells was decreased. Importantly, introducing the *rad53*Δ*sml1*Δ and *rad53*Δ*crt1*Δ mutations into *rad52*Δ cells completely abrogated the elevated oxygen consumption of *rad52*Δ cells. Extremely slow growth of *rad52*Δ*mec1*Δ*sml1*Δ and *rad52*Δ*mec1*Δ*crt1*Δ did not allow culturing these cells in sufficient quantity for further analysis. The oxygen consumption of *dun1*Δ cells was elevated compared with WT cells, and introducing *dun1*Δ mutation into *rad52*Δ cells did not diminish the oxygen consumption of *rad52*Δ cells. This result suggests that induction of respiration in *rad52*Δ cells is not due to degradation of Sml1p and increased dNTP synthesis, because degradation of Sml1p requires Dun1p. The requirement of Rad53p for DDR-induced respiration is consistent with suppression of the elevated ATP levels in *rad52*Δ cells by introducing *rad53*Δ*sml1*Δ and *rad53*Δ*crt1*Δ mutations (Fig. 3*B*).

To corroborate these results, we induced DDR by growing cells bearing deletions of the individual checkpoint kinases in the presence of sublethal concentrations of bleocin. Growth in the presence of bleocin induced respiration in WT, *tel1*Δ, *chk1*Δ, and *dun1*Δ cells. The induction of respiration was completely absent in *mec1*Δ*sml1*Δ, *mec1*Δ*crt1*Δ, *rad53*Δ*sml1*Δ, and *rad53*Δ*crt1*Δ cells (Fig. 3*C*). We interpret these results to mean that Mec1p and its downstream effector kinase Rad53p are required, whereas Tel1p, Chk1p, and Dun1p are not required for DDR-induced respiration. As a control, we also included the *cyt1*Δ strain. *CYT1* encodes cytochrome c_1, and *cyt1*Δ cells are not able to respire (40). The results show that the ETC is responsible for about 95% of the oxygen consumed by the cells growing in the absence or presence of bleocin (Fig. 3*C*).

To test the possibility that the increased oxygen consumption in the WT cells grown in the presence of genotoxic chemicals or in *rad52*Δ cells is caused by a delayed progression through the S phase of the cell cycle, we arrested WT and *rad52*Δ cells in G_1 phase with α-factor and compared oxygen consumption of arrested and asynchronous cells (Fig. 3*D*). Because the oxygen consumption in the two cell populations does not significantly differ for both WT and *rad52*Δ cells, we conclude that the DDR induces respiration in a cell cycle–independent manner.

DDR down-regulates histone levels through activation of Rad53p

Because the connection between DDR and respiration is not immediately obvious and to some extent is counterintuitive, we asked the following question. What is the molecular mechanism underlying this phenomenon? We have recently reported that decreased histone expression results in reduced nucleosome occupancy across the genome and altered chromatin structure, which triggers respiration (40). To determine whether a similar mechanism is responsible for DDR-induced respiration, we assessed histone expression in cells grown in the presence of sublethal concentrations of bleocin or 4-NQO. Under these conditions, the expression of all four histone genes as well as the protein levels of histone H3 were markedly decreased (Fig. 4, *A–C*). A very similar trend of decreased histone gene

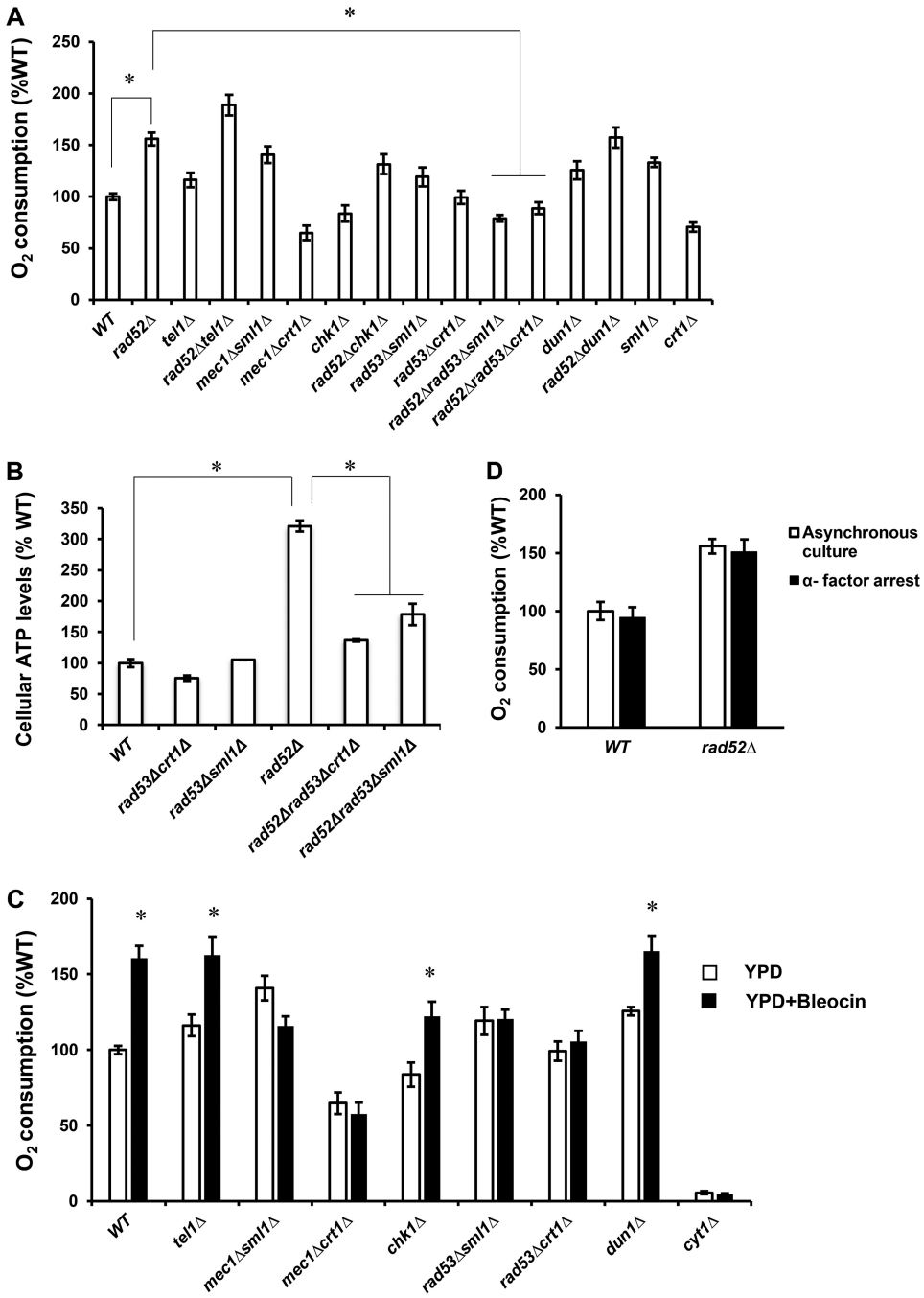

Figure 3. Checkpoint kinases Mec1p and Rad53p are required for DDR-induced respiration. *A, C,* and *D,* cellular oxygen consumption rates; *B,* cellular ATP levels in the indicated strains. *A,* cells were grown in YPD medium, and cellular oxygen consumption was determined in the wildtype (WT, W303-1a), *rad52*Δ (LG731), *tel1*Δ (SN159), *rad52*Δ*tel1*Δ (SN158), *mec1*Δ*sml1*Δ (SN120), *mec1*Δ*crt1*Δ (SN125), *chk1*Δ (SN136), *rad52*Δ*chk1*Δ (SN138), *rad53*Δ*sml1*Δ (LG606), *rad53*Δ*crt1*Δ (LG716), *rad52*Δ*rad53*Δ*sml1*Δ (PB026), *rad52*Δ*rad53*Δ*crt1*Δ (PB019), *dun1*Δ (PB119), *rad52*Δ*dun1*Δ (PB127), *sml1*Δ (LG603), and *crt1*Δ (LG706) cells. *B,* cells were grown in YPD medium, and cellular ATP levels were determined in the wildtype (WT, W303-1a), *rad52*Δ (LG731), *rad53*Δ*sml1*Δ (LG606), *rad53*Δ*crt1*Δ (LG716), *rad52*Δ*rad53*Δ*sml1*Δ (PB026), and *rad52*Δ*rad53*Δ*crt1*Δ (PB019) cells. *A* and *B,* values that are statistically significantly different ($p < 0.05$) from each other are indicated by a *bracket* and an *asterisk*. *C,* cells were grown in YPD medium with or without 0.1 μg/ml bleocin, and the cellular oxygen consumption was determined in the WT (W303-1a), *tel1*Δ (SN159), *mec1*Δ*sml1*Δ (SN120), *mec1*Δ*crt1*Δ (SN125), *chk1*Δ (SN136), *rad53*Δ*sml1*Δ (LG606), *rad53*Δ*crt1*Δ (LG716), and *dun1*Δ (PB119) cells. Values that are statistically significantly different ($p < 0.05$) from the corresponding strain grown in the absence of bleocin are indicated by an *asterisk*. *D,* cell cycle arrest of wildtype (WT, W303-1a) and *rad52*Δ (LG731) cells with α-factor does not affect oxygen consumption. The oxygen consumption of asynchronous and α-factor–treated cells was compared. The α-factor treatment resulted in G_1 arrest of more than 90% cells as unbudded cells. *A–D,* experiments were repeated three times, and the results are shown as means ± S.D. The results are expressed relative to the value for the WT strain.

expression and protein level of histone H3 was observed in *rad52*Δ cells, where the DDR is induced genetically (Fig. 4, *D–H*). Furthermore, down-regulation of histone transcripts and protein levels depended on Rad53p, as introducing *rad53*Δ mutation into *rad52*Δ cells restored histone transcript and protein levels in *rad52*Δ*rad53*Δ*crt1*Δ and *rad52*Δ*rad53*Δ*sml1*Δ cells to the WT levels (Fig. 4, *D–G*). Down-regulation of histone transcripts in *rad52*Δ cells was not suppressed by introducing *tel1*Δ or *dun1*Δ mutations into *rad52*Δ cells and was only partially suppressed by *chk1*Δ mutation.

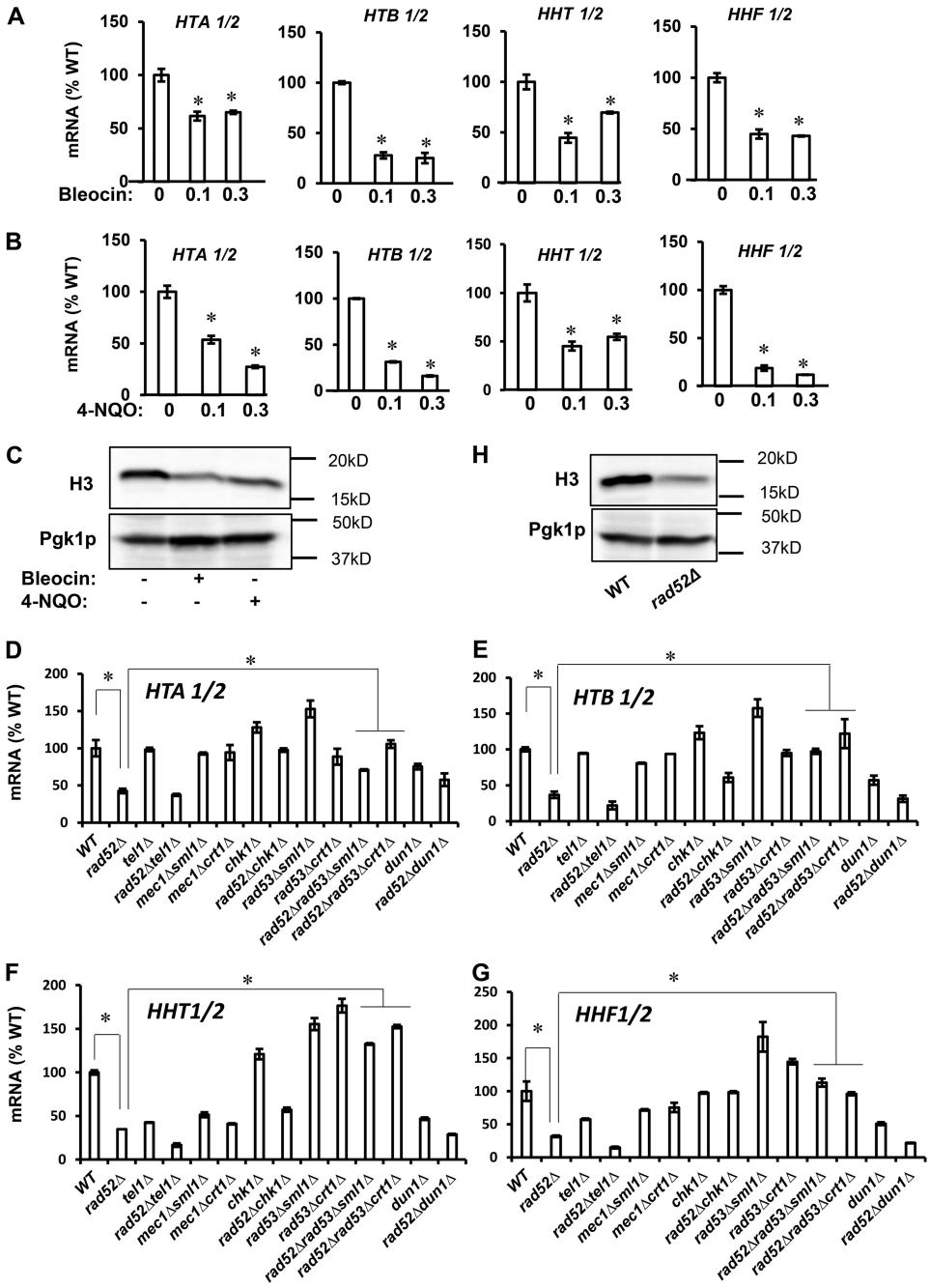

Figure 4. DDR-mediated repression of histone levels requires Rad53p. Transcript levels of core histone genes in WT cells (WT, W303-1a) treated with bleocin at 0, 0.1, and 0.3 μg/ml (*A*) and with 4-NQO at 0, 0.1, and 0.3 μg/ml (*B*). *A* and *B,* values that are statistically significantly different ($p < 0.05$) from the WT cells grown in the absence of bleocin or 4-NQO are indicated by an *asterisk*. *C,* histone H3 protein levels in WT cells grown in the absence of bleocin or 4-NQO, WT cells grown in the presence of 0.3 μg/ml bleocin, and WT cells grown in the presence of 0.1 μg/ml 4-NQO. Transcript levels of histones *HTA1/2* (*D*), *HTB1/2* (*E*), *HHT1/2* (*F*), and *HHF1/2* (*G*) in the wildtype (WT, W303-1a), *rad52*Δ (LG731), *tel1*Δ (SN159), *rad52*Δ*tel1*Δ (SN158), *mec1*Δ*sml1*Δ (SN120), *mec1*Δ*crt1*Δ (SN125), *chk1*Δ (SN136), *rad52*Δ*chk1*Δ (SN138), *rad53*Δ*sml1*Δ (LG606), *rad53*Δ*crt1*Δ (LG716), *rad52*Δ*rad53*Δ*sml1*Δ (PB026), *rad52*Δ*rad53*Δ*crt1*Δ (PB019), *dun1*Δ (PB119), and *rad52*Δ*dun1*Δ (PB127) cells. *D–G,* values that are statistically significantly different ($p < 0.05$) from each other are indicated by a *bracket* and an *asterisk*. *H,* histone H3 protein levels in WT (W303-1a) and *rad52*Δ (LG731) cells. *A, B,* and *D–G,* experiments were repeated three times, and the results are shown as means ± S.D. The results are expressed relative to the value for the WT strain grown in the absence of bleocin or 4-NQO. *C* and *H,* Western blotting analyses were performed three times, and representative results are shown. Pgk1p served as a loading control.

DDR-mediated repression of histone levels alters chromatin structure and induces expression of TCA cycle and ETC genes

Yeast genes can be categorized as growth genes and stress genes, with each group featuring distinct nucleosomal architecture of their promoters (49). The promoter of a growth gene contains a "nucleosome-free region," whereas the promoter of a stress gene is usually occupied by delocalized nucleosomes. As a result, growth genes are constitutively expressed in contrast to stress genes, which are regulated by factors that affect chromatin structure, including abundance of histone proteins. Considering that respiratory genes in *Saccharomyces cerevisiae* belong to the stress gene category (50) and that reduced histone

expression induces respiration (40), we reasoned that by down-regulating histone expression DDR might affect chromatin structure and induce respiratory genes. To test this possibility, we determined histone H3 and RNA pol II occupancy in the promoters of *CIT1*, *IDH1*, and *QCR7*, genes encoding enzymes of the TCA cycle and ETC. The histone H3 occupancy of *CIT1*, *IDH1*, and *QCR7* promoters was significantly reduced in cells treated with bleocin or 4-NQO compared with control cells, whereas the occupancy of RNA pol II at the same set of promoters was increased (Fig. 5, *A* and *B*). Similarly, the histone H3 occupancy of *CIT1*, *IDH1*, and *QCR7* promoters was decreased, whereas RNA pol II occupancy at the same promoters was increased in *rad52*Δ cells (Fig. 5, *C* and *D*). The changes in chromatin structure and RNA pol II occupancy were accompanied by increased transcription of the corresponding genes upon treatment with bleocin or 4-NQO and in *rad52*Δ cells (Fig. 5*E*). In this analysis, we also included the *COX1* gene that is encoded by the mitochondrial genome. As we have shown previously, decreased histone expression and chromatin changes of the nuclear genome affect transcription of genes encoded by the mitochondrial genome. The corresponding mechanism involves elevated expression of nuclear genes *RPO41* and *MTF1*, encoding mitochondrial RNA polymerase and its associated factor, respectively (40).

Inactivation of *RAD52* increased respiration (Fig. 2) and down-regulated histone levels (Fig. 4) in a Rad53p-dependent manner. To determine whether the increased expression of genes required for the TCA cycle, ETC, and OXPHOS in *rad52*Δ cells also requires Rad53p or other checkpoint kinases, we determined transcript levels for *CIT1*, *IDH1*, *QCR7*, and *COX1* genes in *rad52*Δ cells containing deletions of the individual checkpoint kinases (Fig. 6). We found that only inactivation of *RAD53* (in *rad53*Δ*sml1*Δ and *rad53*Δ*crt1*Δ) but not inactivation of *TEL1*, *CHK1*, or *DUN1* suppressed the elevated expression of *CIT1*, *IDH1*, and *QCR7* genes in *rad52*Δ cells.

Elevated histone levels suppress respiration in rad52Δ cells

To test whether the decreased histone levels and altered chromatin structure are indeed responsible for induction of respiration when cells grow in the presence of sublethal concentrations of genotoxic chemicals, we elevated histone levels in WT cells by ectopic expression of extra histones. A high copy number plasmid encoding all four core histones significantly reduced oxygen consumption when cells were grown in the presence of bleocin (Fig. 7, *A* and *B*). In addition, overexpression of histones suppressed oxygen consumption in *rad52*Δ cells (Fig. 7*C*).

In another approach, we tested whether the histone levels can be increased in *rad52*Δ cells by introducing *tom1*Δ or *hir1*Δ mutations. Tom1p functions in a pathway responsible for degradation of free histones. Free histones that are not assembled into chromatin are degraded in a pathway that depends on phosphorylation by Rad53p and ubiquitylation by Ubc4p, Ubc5p, and Tom1p (51, 52). When *TOM1* was deleted in *rad52*Δ cells, the protein level of histone H3 was restored almost to the WT level, confirming the usefulness of this approach (Fig. 7*D*). Hir1p is a subunit of the HIR complex that acts as a histone chaperone and a repressor of the majority of histone genes (53, 54). Inactivation of *HIR1* induces expression of histone genes (35). Introducing *tom1*Δ or *hir1*Δ mutations into *rad52*Δ cells significantly suppressed oxygen consumption, suggesting that it is indeed the decreased level of histones that is responsible for induction of respiration in *rad52*Δ cells (Fig. 7*E*).

DDR-induced respiration activates dNTP synthesis

Does the DDR-induced respiration provide any advantage to yeast cells? One major outcome of DDR is the increase in activity of RNR, the key enzyme that catalyzes the rate-limiting step in dNTP synthesis (16). The complex regulation of RNR activity suggests that the control of the dNTP pools is very important for maintaining genome integrity and cell survival under genotoxic stress. Indeed, the enlargement of dNTP pools is essential for effective DNA repair (14, 15).

In our previous work, we have shown that reduced histone expression and altered chromatin structure induce respiration and significantly elevate cellular ATP levels (40). To determine whether increased respiration and elevated ATP levels can drive up dNTP synthesis, we evaluated the sizes of dNTP pools in *swi6*Δ and *asf1*Δ cells (Fig. 8*A*). Swi6p is the transcriptional activation subunit of the SBF and MBF complexes that regulate histone gene transcription (35, 36). Asf1p is a histone chaperone involved in chromatin assembly. Both *swi6*Δ and *asf1*Δ cells display markedly up-regulated oxygen consumption and ATP levels (40). We found that the dNTP pools are significantly increased in *swi6*Δ and *asf1*Δ cells, and the increase is abolished in *swi6*Δ*cyt1*Δ and *asf1*Δ*cyt1*Δ cells (Fig. 8*A*). *CYT1* encodes the cytochrome c_1 subunit, and deletion of *CYT1* inactivates the ETC. When we induced DDR in WT cells either chemically or genetically, the dNTP pools were also significantly increased. However, blocking respiration by introducing the *cyt1*Δ mutation appreciably decreased dNTP levels in *rad52*Δ cells or WT cells treated with bleocin or 4-NQO (Fig. 8*B*). These results indicate that decreased histone expression and the defect in chromatin structure or growth in the presence of genotoxic chemicals activate respiration and increase ATP and dNTP levels.

Survival of yeast cells in the presence of DNA damage depends on the availability of dNTPs for effective DNA repair (14, 19). Consistently with this role of increased dNTP pools for effective DNA repair, *cyt1*Δ cells that cannot up-regulate respiration and are thus unable to effectively enlarge their dNTP pools are more sensitive to bleocin or hydroxyurea (Fig. 8*C*). Inactivation of *SML1* does not significantly change growth on bleocin or hydroxyurea, but *sml1*Δ*cyt1*Δ cells are more sensitive to bleocin or hydroxyurea than *sml1*Δ cells. Interestingly, *sml1*Δ*cyt1*Δ cells appear to be more sensitive to hydroxyurea than *cyt1*Δ cells. The difference in sensitivity to hydroxyurea between *cyt1*Δ and *sml1*Δ*cyt1*Δ cells is quite subtle but reproducible. Because both ATP and Sml1p are allosteric regulators of RNR (55), this observation may indicate that under conditions of direct inhibition of RNR by hydroxyurea, the absence of Sml1p sensitizes RNR to low ATP levels.

To test whether the lethality of *rad53*Δ mutation can be suppressed by increasing dNTP synthesis by up-regulating respiration and ATP synthesis, we introduced *mbp1*Δ mutation into *rad53*Δ cells. *MBP1* encodes the DNA-binding subunit of the

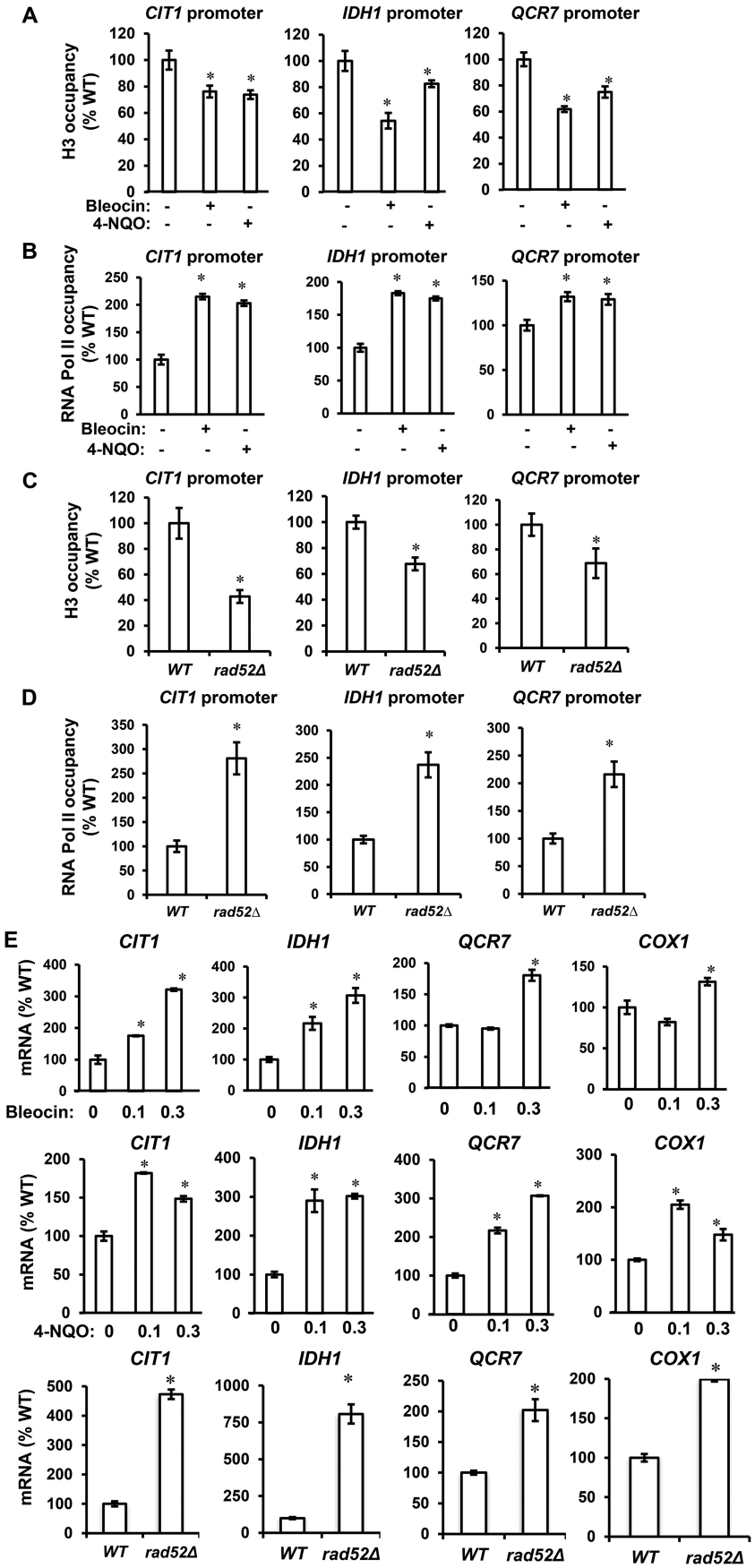
A
CIT1 promoter
IDH1 promoter
QCR7 promoter
H3 occupancy (% WT)
Bleocin:
4-NQO:
B
RNA Pol II occupancy (% WT)
C
H3 occupancy (% WT)
WT
rad52Δ
D
RNA Pol II occupancy (% WT)
E
CIT1
IDH1
QCR7
COX1
mRNA (% WT)
Bleocin: 0 0.1 0.3
4-NQO: 0 0.1 0.3

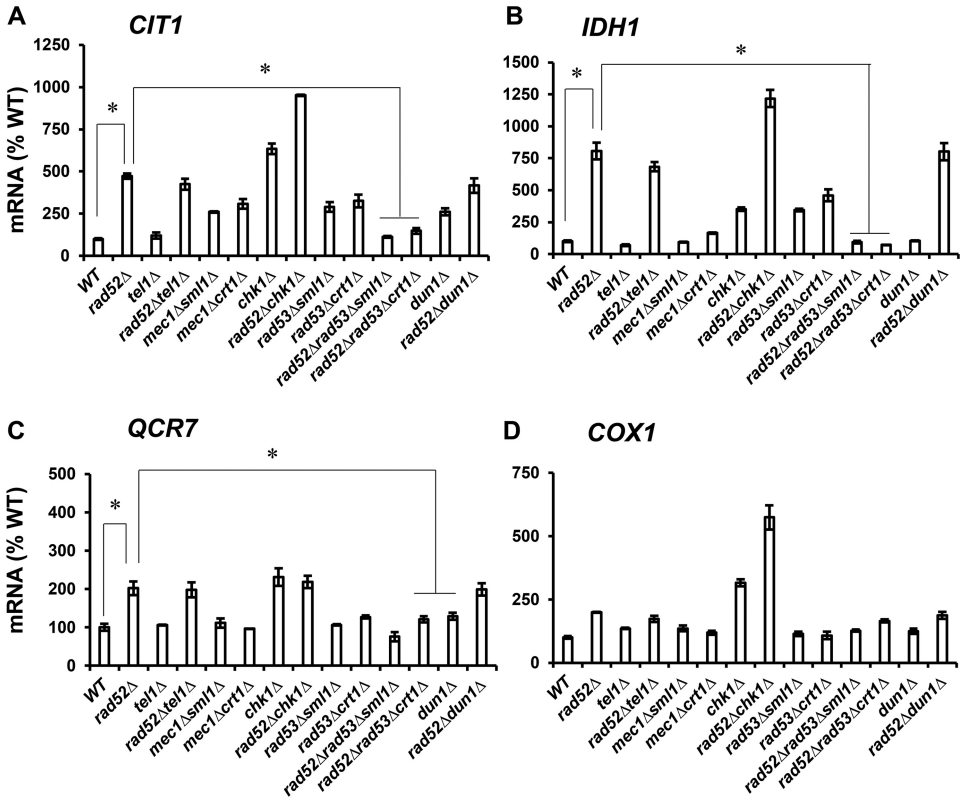

Figure 6. DDR-mediated induction of TCA cycle and ETC genes requires Rad53p. Transcript levels of *CIT1* (*A*), *IDH1* (*B*), *QCR7* (*C*), and *COX1* (*D*) in the WT (W303-1a), *rad52*Δ (LG731), *tel1*Δ (SN159), *rad52*Δ*tel1*Δ (SN158), *mec1*Δ*sml1*Δ (SN120), *mec1*Δ*crt1*Δ (SN125), *chk1*Δ (SN136), *rad52*Δ*chk1*Δ (SN138), *rad53*Δ*sml1*Δ (LG606), *rad53*Δ*crt1*Δ (LG716), *rad52*Δ*rad53*Δ*sml1*Δ (PB026), *rad52*Δ*rad53*Δ*crt1*Δ (PB019), *dun1*Δ (PB119), and *rad52*Δ*dun1*Δ (PB127) cells. The experiments were repeated three times, and the results are shown as means ± S.D. relative to the value for the WT strain. *A–C,* values that are statistically significantly different ($p < 0.05$) from each other are indicated by a *bracket* and an *asterisk*.

MBF transcriptional factor. We have shown previously that *mbp1*Δ cells display increased respiration and ATP levels (40). The *rad53*Δ*mbp1*Δ cells are viable and grow significantly better than the *rad53*Δ*mbp1*Δ*cyc1*Δ cells (Fig. 8*D*). *CYC1* encodes cytochrome *c*, and *cyc1*Δ cells are not able to respire (56). This result indicates that increasing respiration and presumably ATP and dNTP synthesis represent the major mechanism for suppression of *rad53*Δ lethality by *mbp1*Δ mutation.

Only long-term but not acute genotoxic stress induces respiration

Several studies found that DDR represses transcription of genes encoding enzymes of the TCA cycle, ETC, and OXPHOS. These studies evaluated acute exogenous genotoxic stress, typically created by 1–2-h cell exposure to genotoxic chemicals (37, 60). In contrast, our results show that chronic activation of DDR rendered by *rad52*Δ mutation or by growing WT cells in the presence of sublethal concentrations of genotoxic chemicals activates transcription of the TCA cycle, ETC, and OXPHOS genes and elevates oxygen consumption. To determine whether the duration of the genotoxic stress is responsible for the difference between our results and studies that found the inhibitory effect of DDR on transcription of respiratory genes (37, 60), we performed a time-course experiment and measured oxygen consumption and transcription of *CIT1*, *IDH1*, *QCR7*, and *COX1* genes for several hours after addition of bleocin (Fig. 9). Indeed, the most significant increase in oxygen consumption (Fig. 9*A*) and transcription of the respiratory genes (Fig. 9*B*) is observed after more than 2 h of growth in the presence of bleocin. These results show that increased respiration is a long-term response to a chronic sublethal genotoxic stress and suggest that long-term survival and growth under chronic genotoxic stress requires increased respiration to support ATP and dNTP synthesis.

Discussion

The key finding of this study is that the DDR activates respiration to increase ATP production and elevate dNTP levels, which are required for efficient DNA repair. Based on our results, we propose a model in which DDR regulates dNTP

Figure 5. DDR-mediated repression of histone levels alters chromatin structure and induces expression of TCA cycle and ETC genes. ChIP-qPCR analysis of histone H3 (*A*) and RNA polymerase II (*B*) occupancy at *CIT1*, *IDH1*, and *QCR7* promoters in WT cells (WT, W303-1a) grown in the absence of bleocin or 4-NQO, WT cells grown in the presence of 0.3 μg/ml bleocin, and WT cells grown in the presence of 0.1 μg/ml 4-NQO is shown. ChIP-qPCR analysis of histone H3 (*C*) and RNA polymerase II (*D*) occupancy at *CIT1*, *IDH1*, and *QCR7* promoters in WT and *rad52*Δ cells is shown. *E,* transcript levels of *CIT1*, *IDH1*, *QCR7*, and *COX1* genes in WT cells grown in the absence of bleocin or 4-NQO, WT cells grown in the presence of 0.3 μg/ml bleocin, and WT cells grown in the presence of 0.1 μg/ml 4-NQO. The *bottom row* shows transcript levels of the indicated genes in WT and *rad52*Δ (LG731) cells. The experiments were repeated three times, and the results are shown as means ± S.D. Values that are statistically significantly different ($p < 0.05$) from the WT cells are indicated by an *asterisk*. The results are expressed relative to the value for the WT strain grown in the absence of bleocin or 4-NQO.

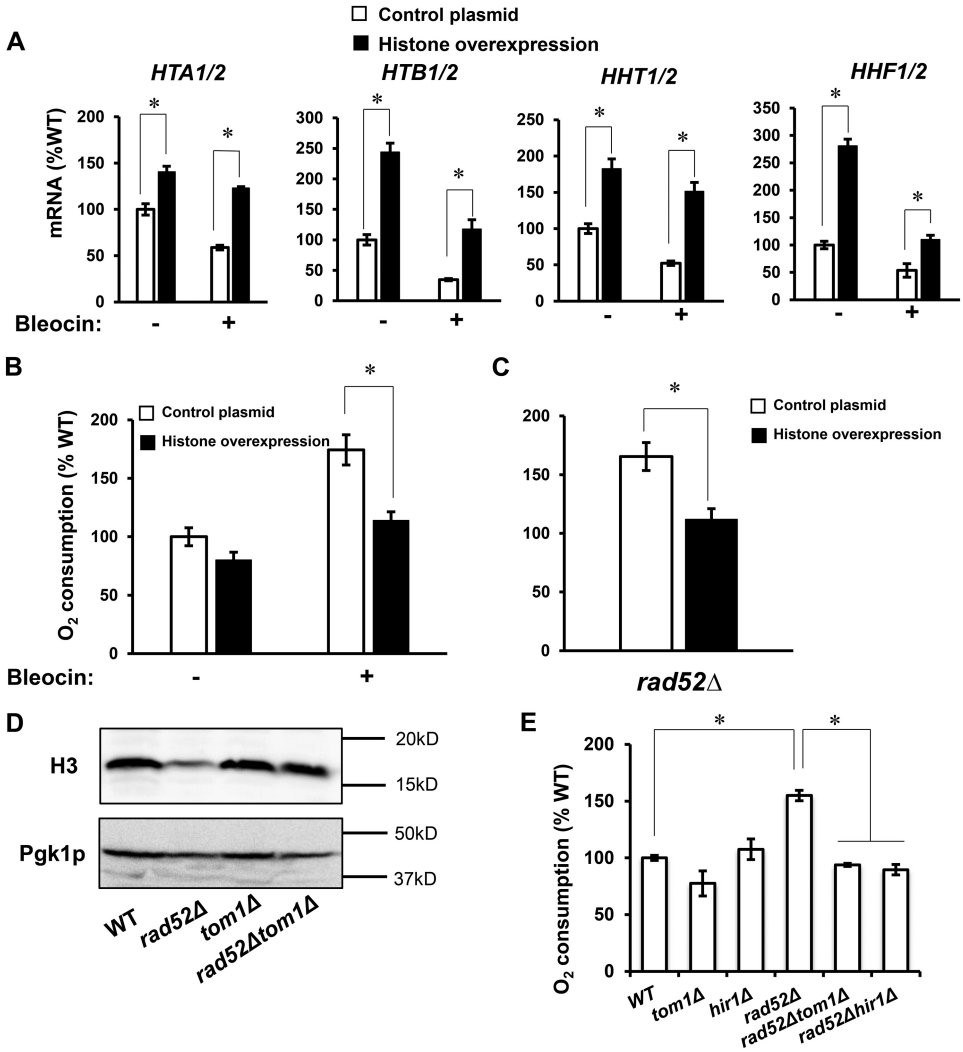

Figure 7. Elevated histone levels suppress DDR-induced respiration. Relative mRNA levels of histone genes (*A*) and oxygen consumption rate (*B*) of WT cells (WT, W303-1a) containing either control plasmid or high copy number plasmid expressing all four core histone genes (plasmid pRS426-HTA1/HTB1-HHF1/HHT1). The cells were pre-grown under selection in SC medium and inoculated to an $A_{600\ nm}$ of 0.1 into YPD medium containing 0 or 0.3 μg/ml of bleocin and grown for two generations at 30 °C. *C,* oxygen consumption rate of *rad52*Δ (LG731) cells containing either control plasmid or plasmid pRS426-HTA1/HTB1-HHF1/HHT1. The cells were pre-grown under selection in SC medium and inoculated to an $A_{600\ nm}$ of 0.1 into YPD medium and grown for two generations. *D,* histone H3 protein levels in the wildtype (WT, W303-1a), *rad52*Δ (LG731), *tom1*Δ (LG734), and *rad52*Δ*tom1*Δ (LG774) cells. Western blotting analyses were performed three times, and representative results are shown. Pgk1p served as a loading control. *E,* oxygen consumption rate in the WT (W303-1a), *rad52*Δ (LG731), *tom1*Δ (LG734), *rad52*Δ*tom1*Δ (LG774), *hir1*Δ (MZ700), and *rad52*Δ*hir1*Δ (PB066) cells. *A–C* and *E,* experiments were repeated three times, and the results are shown as means ± S.D. Values that are statistically significantly different ($p < 0.05$) from each other are indicated by a *bracket* and an *asterisk*. The results are expressed relative to the value for the WT strain.

synthesis by a bifurcating mechanism (Fig. 10). In one well-established branch of the pathway, Dun1p inactivates Crt1p, Sml1p, and Dif1p, leading to increased RNR activity and dNTP synthesis (31–34). In the second branch of the pathway, Mec1p and Rad53p down-regulate transcription of histone genes (Fig. 10). Decreased histone levels result in altered chromatin structure and induction of TCA cycle and ETC genes required for respiration (40). A direct outcome of elevated respiration is increased production of ATP, a potent allosteric activator for the RNR enzyme (16, 18), increased synthesis of dNTPs, and improved cell survival (Fig. 10). This "histone" branch of the pathway does not require Dun1p and inactivation of Crt1p, Sml1p, and Dif1p, because inducing DDR in *dun1*Δ cells activates respiration almost to the same level as in the WT cells (Fig. 3, *A* and *C*).

Based on chromatin architecture, yeast genes belong to one of two broad groups: growth genes and stress genes (49). Growth genes are expressed rather constitutively, and their promoters feature a nucleosome-free region where transcription factors bind upstream of the ORF. Stress genes are expressed at a lower level, and their promoters are dominated by delocalized nucleosomes rather than by the nucleosome-free region. Consequently, stress genes are regulated by factors that affect the structure of chromatin, including histone level. The respiratory genes in *S. cerevisiae* belong to the stress category, unlike respiratory genes in higher eukaryotes (50). Consequently, reduced histone expression or a defect in chromatin assembly induces respiration by allowing increased activation of the TCA cycle, ETC, and OXPHOS genes by the Hap2/3/4/5p complex (40).

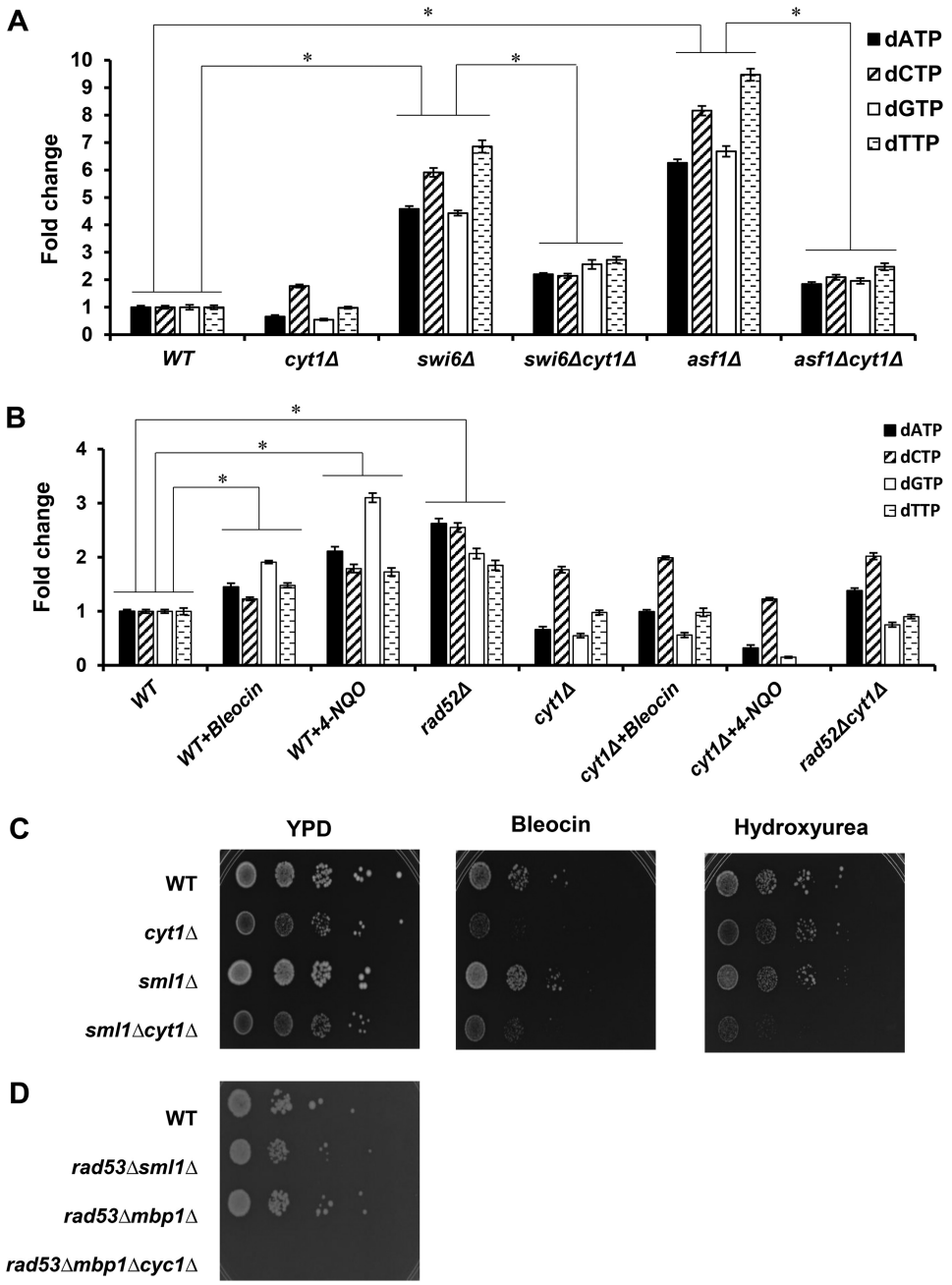

Figure 8. DDR-induced respiration activates dNTP synthesis and improves cell survival upon DNA damage. *A,* cellular dNTP levels in the wildtype (WT, W303-1a), *cyt1*Δ (LG533), *swi6*Δ (DY5780), *swi6*Δ*cyt1*Δ (LG567), *asf1*Δ (MZ576), and *asf11*Δ*cyt1*Δ (LG570) cells. *B,* cellular dNTP levels in the wildtype (WT, W303-1a), *rad52*Δ (LG731), and *cyt1*Δ (LG533) cells grown in YPD medium and WT cells grown in YPD medium containing 0.3 μg/ml bleocin or 0.1 μg/ml 4-NQO. *A* and *B,* experiments were repeated three times, and the results are shown as means ± S.D. Individual dNTP levels are expressed relative to the corresponding dNTP in the WT cells grown in the absence of bleocin or 4-NQO. Strains with all four dNTP levels statistically significantly different from each other are indicated by a *bracket* and an *asterisk*. *C,* 10-fold serial dilutions of the wildtype (WT, W303-1a), *cyt1*Δ (LG533), *sml1*Δ (LG603), and *sml1*Δ*cyt1*Δ (PB061) cells were spotted onto YPD plates, YPD plates containing 0.1 μg/ml bleocin, or YPD plates containing 150 mM hydroxyurea and grown for 3 days. *D,* electron transport chain is required for suppression of *rad53*Δ lethality by *mbp1*Δ mutation. The 10-fold serial dilutions of the wildtype (WT, W303-1a), *rad53*Δ*sml1*Δ (LG606), *rad53*Δ*mbp1*Δ (MB051), and *rad53*Δ*mbp1*Δ*cyc1*Δ (MB054) cells were spotted onto YPD plates and grown for 2 days. *C* and *D,* typical results from three independent experiments are shown.

Although it is well-established that DNA replication is coordinated with transcription of histone genes and that DDR represses histone transcription, the role of Rad53p in this process is not fully understood. The expression of histone genes is regulated by two G_1/S-specific transcription complexes SBF and MBF, in addition to other transcription regulators (35, 36). Swi4p/Swi6p and Mbp1p/Swi6p form SBF and MBF, respectively. DDR induces Rad53p-dependent phosphorylation of Swi6p, which results in down-regulation of *CLN1* and *CLN2* transcription and delayed G_1 to S progression (58, 59). On the other hand, Rad53p phosphorylates and inactivates Nrm1p, the co-repressor of MBF, which results in activation of MBF targets (23, 24). Systematic phosphoproteomics screen identified Swi6p, Swi4p, and Mbp1p as direct targets of Rad53p (60).

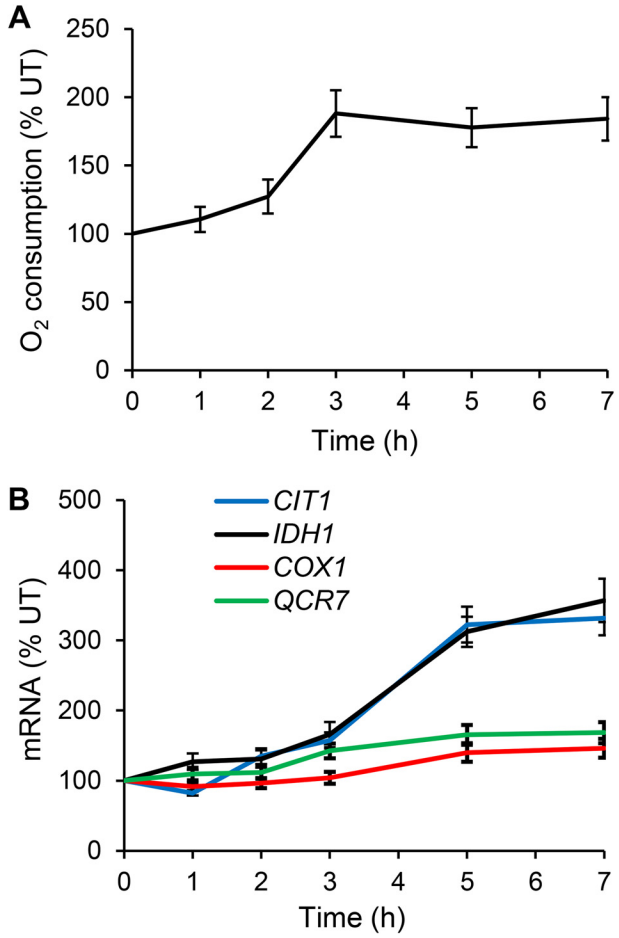

Figure 9. Long-term but not acute genotoxic stress induces respiration. Cellular oxygen consumption rate (*A*) and transcript levels of *CIT1*, *IDH1*, *QCR7*, and *COX1* genes (*B*) in WT cells (WT, W303-1a) grown in YPD medium containing 0.3 μg/ml bleocin. The culture was maintained in early exponential phase (below $A_{600\,nm} = 0.6$) by diluting with pre-warmed YPD medium containing 0.3 μg/ml bleocin. The experiments were repeated three times, and the results are shown as means ± S.D. The results are expressed relative to the value for untreated (*UT*) WT strain.

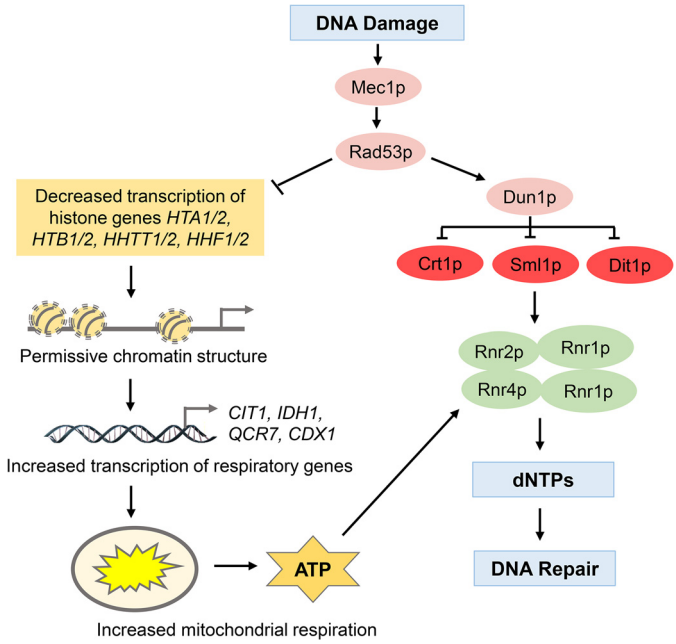

Figure 10. Model depicting DDR-induced respiration. DDR, in a Mec1p- and Rad53p-dependent way, regulates dNTP synthesis by a bifurcating mechanism. In one well-established branch of the pathway, Dun1p inactivates Crt1p, Sml1p, and Dif1p, leading to increased RNR activity and dNTP synthesis. In the second branch of the pathway, Mec1p and Rad53p down-regulate transcription of histone genes. Decreased histone levels result in altered chromatin structure and induction of TCA cycle and ETC genes required for respiration. A direct outcome of elevated respiration is increased production of ATP, a potent allosteric activator for the RNR enzyme, increased synthesis of dNTPs, and improved cell survival.

Because the transcription of the histone genes is reduced in *swi4*Δ and *mbp1*Δ cells (61), the simplest explanation for the role of Rad53p in regulation of histone gene transcription is that Rad53p phosphorylates and down-regulates SBF and MBF complexes.

How does elevated respiration and ATP levels regulate dNTP synthesis? The large subunit of both mammalian and yeast RNR contains the catalytic site as well as two allosteric sites (16, 17, 19). One of the allosteric sites, the "specificity site," binds dTTP, dGTP, and dATP and regulates the appropriate ratios among the four dNTP pools. The second allosteric site, the "activity site," binds ATP or dATP and regulates the total dNTP pool size by monitoring the dATP/ATP ratio. When the cellular ATP-to-dATP ratio increases, the binding of ATP to this allosteric site activates RNR, promoting synthesis of all dNTPs. When the dNTP concentration reaches a certain level, the RNR activity is allosterically inhibited by binding of dATP to the "activity site." DNA replication fidelity requires correct absolute and relative concentrations of the dNTPs (62, 63), and mutations in both the "specificity" and "activity" sites of yeast RNR result in significantly reduced replication fidelity (14, 63).

In yeast RNR, the allosteric dATP feedback inhibition is more relaxed, allowing the increase of dNTP pools upon DNA damage (14). The increase in dNTP pools significantly improves survival following DNA damage; however, it also results in higher mutation rates (14, 57, 64). Our results suggest that the DDR-induced expansion of the dNTP pools is partly facilitated by elevated respiration and ATP production.

The relationship between respiratory metabolism and DNA replication and repair is contentious. Leakage of electrons from the ETC is one of the endogenous sources of ROS, which damage cellular structures, including DNA, contributing to the pathogenesis of cardiovascular diseases, inflammatory diseases, and cancer, and a shorter life span (65, 66). However, mitochondria can also function as a cellular antioxidant defense, and increased mitochondrial activity enables more efficient operation of the ETC, limiting ROS production and increasing antioxidant capacity (67). In addition, DNA replication and repair are energetically costly (45), and ETC and OXPHOS generate significantly more ATP than glycolysis. This energetic aspect of DNA repair is evolutionarily conserved, as illustrated by increased fatty acid oxidation, oxidative phosphorylation, and oxygen consumption in response to both chronic endogenous and acute exogenous genotoxic stress in mice (68).

DNA damage induced by methylmethane sulfonate (MMS) was reported to suppress respiration (69), down-regulate yeast AMP-activated protein kinase ortholog Snf1p (43), and suppress transcription of genes regulated by the Hap1p and Hap2/3/4/5p complex (37, 60). Hap1p and Hap2/3/4/5p activate genes encoding enzymes of the TCA cycle, ETC, and OXPHOS.

The repression of Hap1p and Hap2/3/4/5p targets was independent of checkpoint kinases and was not observed in cells exposed to ionizing radiation (37). The authors concluded that the MMS-induced repression of Hap1p and Hap2/3/4/5p targets was not specific for DNA damage and was a consequence of oxidative stress or other effect of MMS on Hap1p and Hap2/3/4/5p signaling (37, 60). These results are in agreement with our observations. When we tested different genotoxic chemicals for respiration inducers, we also included MMS. Even with MMS concentrations spanning from 0.0001 to 0.01%, we could not detect any stimulatory effect on oxygen consumption, although we observed consistent and marked stimulation of oxygen consumption in cells treated with bleocin or 4-NQO (Fig. 2). We conclude that the effect of MMS on respiration is not representative of genotoxic chemicals and DDR but rather reflects the particular properties of MMS and/or the specific pathways MMS affects. This conclusion is supported by direct inhibition of respiration in isolated mitochondria by MMS (69).

This study connects respiratory metabolism and DDR, two processes deemed not to be very compatible. We speculate that the benefit of increased ATP and dNTP synthesis for cell survival offsets the deleterious effect of respiratory metabolism on DNA repair.

Materials and methods

Yeast strains, media, and plasmid construction

All yeast strains used in this study are listed in Table 2. Standard genetic techniques were used to manipulate yeast strains and to introduce mutations from non-W303 strains into the W303 background (71). Cells were grown at 30 °C in yeast extract/peptone/dextrose (YPD) medium containing 2% glucose or under selection in synthetic complete medium containing 2% glucose and, when appropriate, lacking specific nutrients to select for a particular genotype. Cell cycle arrest in G_1 phase by α-factor was carried out by adding α-factor to 10 μg/ml to cells exponentially growing in YPD medium. Following α-factor addition, the cultures were incubated for 3 h, and the arrest was monitored by examining cell morphology (72). For construction of plasmid pRS426-HTA1/HTB1–HHF1/HHT1, the *HTA1/HTB1* locus was amplified by PCR using forward primer 5′-TTCACACGAGCGAATTCTCTGAAG-3′ and reverse primer 5′-AGCAACAGTGCTCGAGGAACCTAA-3′. The *HHF1–HHT1* locus was amplified using forward primer 5′-AAATACGAGCTCCGTGTAAGTTACAGAC-3′ and reverse primer 5′-TTTCGAGGGGATCCCCAGGAAAA-3′. The *HHF1–HHT1* fragment was digested with SacI and BamHI and ligated into pRS426. The *HTB1–HTA1* fragment was digested with EcoRI and XhoI and ligated into the pRS426-HTA1/HTB1 plasmid.

Oxygen consumption measurement

Oxygen consumption measurements were performed essentially as described (40, 46). Cells were grown to an $A_{600\ nm}$ of 0.6 in YPD medium containing 2% glucose, and 3 $A_{600\ nm}$ units (9×10^7) of yeast cells were harvested by centrifugation. Cells were resuspended in a buffer containing 10 mM HEPES, 25 mM K_2HPO_4, pH 7.0, and incubated at 30 °C in an oxygen consumption chamber (Instech Laboratories, Inc.) connected to a NeoFOX fluorescence-sensing detector using NeoFOX software (Ocean Optics, Inc.). Results were calculated as picomoles of $O_2/10^6$ cells/s and expressed as percentages of the WT value. The oxygen consumption rate in WT cells grown in YPD medium was 5.08 pmol/10^6 cells/s and was set as 100%.

Cellular ATP assays

Cellular ATP levels were determined as described (40, 46). Cells were grown to an $A_{600\ nm}$ of 0.6 in YPD medium containing 2% glucose, and 3 $A_{600\ nm}$ units (9×10^7) of yeast cells were harvested, and cells were harvested by centrifugation and lysed in 5% TCA with pre-chilled glass beads. Cell lysate was neutralized to pH 7.5 with 10 M KOH and 2 M Tris-HCl, pH 7.5. ATP levels were measured using the ENLITEN ATP assay (FF2000, Promega) according to the manufacturer's instructions and normalized by the number of cells. The ATP level in WT cells grown on YPD medium was 0.58 μmol/10^{10} cells and was set as 100%.

RNA extraction and real-time RT-qPCR

The procedures to extract total RNA from yeast cells and perform real-time RT-qPCR were as described previously (73). The primers used are as follows: *ACT1* (5′-TATGTGTAAAGCCGGTTTTGC-3′ and 5′-GACAATACCGTGTTCAATTGGG-3′); *CIT1* (5′-CAGCGATATTATCAACAACTAGCA-3′ and 5′-TAGTGGCGAGCATTCAATAGTG-3′); *IDH1* (5′-TGCTTAACAGAACAATTGCTAAGAG-3′ and 5′-AACACCGTCACCAGGTATCAA-3′); *QCR7* (5′-ACGTCTATTGCGAGAATTGGTG-3′ and 5′-AGCCCTAACTTCTTGTAACCTGC-3′); and *COX1* (5′-CAACAAATGCAAAAGATATTGCAG-3′ and 5′-AATATTGTGAACCAGGTGCAGC-3′). The histone gene primers recognize both copies of the core histone gene: *HTA1/2* (5′-CGGTGGTAAAGGTGGTAAAGC-3′ and 5′-TGGAGCACCAGAACCAATTC-3′); *HTB1/2* (5′-CAAAGTTTTGAAGCAAACTCACCC-3′ and 5′-GCCAATTTAGAAGCTTCAGTAGC-3′); *HHT1/2* (5′-GAAGCCTCACAGATATAAGCCAG-3′ and 5′-ATCTTGAGCGATTTCTCTGACC-3′); and *HHF1/2* (5′-CCAAGCGTCACAGAAAGATTCTA-3′ and 5′-ACCAGAAATACGCTTGACACCA-3′).

Western blotting

Whole-cell lysates were prepared, and Western blotting was performed as described previously (40). Briefly, cells were grown in YPD medium containing 2% glucose to an $A_{600\ nm}$ of 0.6. Four $A_{600\ nm}$ units (1 $A_{600\ nm}$ unit is equal to 3×10^7 cells) of yeast cells were harvested and immediately boiled in SDS sample buffer. Anti-histone H3 polyclonal antibody (Abcam, ab1791) was used at a dilution of 1:1000, and anti-Pgk1p (Invitrogen, 459250) was used at a dilution of 1:3000.

ChIP-qPCR

In vivo chromatin cross-linking and immunoprecipitation were performed essentially as described (73). Immunoprecipitation was performed with ChIP grade anti-histone H3 antibody (Abcam, ab1791) and anti-RNA polymerase II antibody (Abcam, ab817). The primers used for qPCR are as follows: *POL1* (5′-TCCTGACAAAGAAGGCAATAGAAG-3′ and 5′-

Table 2
Yeast strains used in this study

Strain	Genotype	Source/Ref.
W303-1a	*MATa ade2-1 his3-11,15 leu2-3,112 trp1-1 ura3-1 ssd1-d2 can1-100*	R. Rothstein
W303-1α	*MATα ade2-1 his3-11,15 leu2-3,112 trp1-1 ura3-1 ssd1-d2 can1-100*	R. Rothstein
W303	*MATa/MATα ade2-1/ade2-1 his3-11,15/his3-11,15 leu2-3,112/leu2-3,112 trp1-1/trp1-1ura3-1/ura3-1 can1-100/can1-100*	R. Rothstein
LG716	*MATa ade2-1 his3-11,15 leu2-3,112 trp1-1 ura3-1 ssd1-d2 can1-100 rad53::KAN crt1::LEU2*	This study
LG606	*MATa ade2-1 his3-11,15 leu2-3,112 trp1-1 ura3-1 ssd1-d2 can1-100 rad53::KAN sml1::HYG*	This study
LG731	*MATa ade2-1 his3-11,15 leu2-3,112 trp1-1 ura3-1 ssd1-d2 can1-100 rad52::TRP1*	This study
PB019	*MATa ade2-1 his3-11,15 leu2-3,112 trp1-1 ura3-1 ssd1-d2 can1-100 rad52::TRP1 rad53::KAN crt1::LEU2*	This study
PB026	*MATa ade2-1 his3-11,15 leu2-3,112 trp1-1 ura3-1 ssd1-d2 can1-100 rad52::TRP1 rad53::KAN sml1::HYG*	This study
LG734	*MATa ade2-1 his3-11,15 leu2-3,112 trp1-1 ura3-1 ssd1-d2 can1-100 tom1::TRP1*	This study
MZ700	*MATa ade2-1 his3-11,15 leu2-3,112 trp1-1 ura3-1 ssd1-d2 can1-100 hir1::HIS3*	40
LG774	*MATa ade2-1 his3-11,15 leu2-3,112 trp1-1 ura3-1 ssd1-d2 can1-100 rad52::TRP tom1::TRP1*	This study
PB066	*MATa ade2-1 his3-11,15 leu2-3,112 trp1-1 ura3-1 ssd1-d2 can1-100 rad52::TRP hir1::HIS3*	This study
LG533	*MATa ade2-1 his3-11,15 leu2-3,112 trp1-1 ura3-1 ssd1-d2 an1-100 cyt1::KAN*	40
PB051	*MATa ade2-1 his3-11,15 leu2-3,112 trp1-1 ura3-1 ssd1-d2 can1-100 rad52::TRP1 cyt1::KAN*	This study
DY5780	*MATa ade2-1 his3-11,15 leu2-3,112 trp1-1 ura3-1 ssd1-d2 can1-100 swi6::TRP1*	70
LG567	*MATa ade2-1 his3-11,15 leu2-3,112 trp1-1 ura3-1 ssd1-d2 can1-100 swi6::TRP1 cyt1::KAN*	40
MZ576	*MATa ade2-1 his3-11,15 leu2-3,112 trp1-1 ura3-1 ssd1-d2 can1-100 asf1::HIS3*	40
LG570	*MATa ade2-1 his3-11,15 leu2-3,112 trp1-1 ura3-1 ssd1-d2 can1-100 asf1::HIS3 cyt1::KAN*	40
FY2771	*MATa his3Δ200 ura3Δ0 leu2Δ0 lys2-128δ mec1::HIS3 sml1::KAN*	39
SN117	*MATa ade2-1 his3-11,15 leu2-3,112 trp1-1 ura3-1 ssd1-d2 can1-100 mec1::HIS3 sml1::KAN*	This study
SN120	*MATa ade2-1 his3-11,15 leu2-3,112 trp1-1 ura3-1 ssd1-d2 can1-100 rad52::TRP1 mec1::HIS3 sml1::KAN*	This study
SN125	*MATα ade2-1 his3-11,15 leu2-3,112 trp1-1 ura3-1 ssd1-d2 can1-100 mec1::HIS3 crt1::LEU2*	This study
SN133	*MATa ade2-1 his3-11,15 leu2-3,112 trp1-1 ura3-1 ssd1-d2 can1-100 rad52::TRP1 mec1::HIS3 crt1::LEU2*	This study
RDKY3731	*MATa ura3-52 leu2Δ1 trp1Δ63 his3Δ200 lys2ΔBgl hom3-10 ade2Δ1 ade8 hxt13::URA3 tel1::HIS3*	41
SN159	*MATa ade2-1 his3-11,15 leu2-3,112 trp1-1 ura3-1 ssd1-d2 can1-100 tel1::HIS3*	This study
SN158	*MATα ade2-1 his3-11,15 leu2-3,112 trp1-1 ura3-1 ssd1-d2 can1-100 rad52::TRP1 tel1::HIS3*	This study
RDKY3745	*MATa ura3-52 leu2Δ1 trp1Δ63 his3Δ200 lys2ΔBgl hom3-10 ade2Δ1 ade8 hxt13::URA3 chk1::HIS3*	41
SN136	*MATα ade2-1 his3-11,15 leu2-3,112 trp1-1 ura3-1 ssd1-d2 can1-100 chk1::HIS3*	This study
SN138	*MATα ade2-1 his3-11,15 leu2-3,112 trp1-1 ura3-1 ssd1-d2 can1-100 rad52::TRP1 chk1::HIS3*	This study
RDKY3739	*MATa ura3-52 leu2Δ1 trp1Δ63 his3Δ200 lys2ΔBgl hom3-10 ade2Δ1 ade8 hxt13::URA3 dun1::HIS3*	41
cyc1::URA3	*MATa ade2-1 his3-1,15 leu2-3,112 trp 1-1 ura3-1 cyc1::URA3*	56
SN102	*MATa ade2-1 his3-11,15 leu2-3,112 trp1-1 ura3-1 ssd1-d2 can1-100 dun1::HIS3 cyt1::KAN*	This study
LG603	*MATa ade2-1 his3-11,15 leu2-3,112 trp1-1 ura3-1 ssd1-d2 can1-100 sml1::HYG*	This study
PB061	*MATa ade2-1 his3-11,15 leu2-3,112 trp1-1 ura3-1 ssd1-d2 can1-100 sml1::HYG cyt1::KAN*	This study
PB119	*MATa ade2-1 his3-11,15 leu2-3,112 trp1-1 ura3-1 ssd1-d2 can1-100 dun1::KAN*	This study
PB127	*MATa ade2-1 his3-11,15 leu2-3,112 trp1-1 ura3-1 ssd1-d2 can1-100 rad52::TRP1 dun1::KAN*	This study
LG706	*MATa ade2-1 his3-11,15 leu2-3,112 trp1-1 ura3-1 ssd1-d2 can1-100 crt1::LEU2*	This study
MB051	*MATa ade2-1 his3-11,15 leu2-3,112 trp1-1 ura3-1 ssd1-d2 can1-100 rad53::KAN mbp1::TRP1*	This study
MB054	*MATa ade2-1 his3-11,15 leu2-3,112 trp1-1 ura3-1 ssd1-d2 can1-100 rad53::KAN mbp1::TRP1 cyc1::URA3*	This study

TAAAACACCCTGATCCACCTCTG-3′); *CIT1* (5′-CCTTTGGAGCTTTTCCGATA and 5′-GCAAATTTCCCCCTTAAGAC-3′); *IDH1* (5′-AGCGATTAAAGGAAGACCCTC-3′ and 5′-CTACGGTAGAGTAAAGAAATC-3′); and *QCR7* (5′-ACAGCAGGCCAAAAACCAA-3′ and 5′-AAAGTAAATTGTCAGGCCCCC-3′).

dNTP quantitative analysis

Four $A_{600\,nm}$ units (12×10^7) of yeast cells were harvested and lysed in 5% TCA with pre-chilled glass beads. Cell lysate was neutralized to pH 7.5 with 10 M KOH and 2 M Tris-HCl, pH 7.5. The lysate was used immediately for probe-based quantitative PCR analysis of individual dNTP levels or aliquoted and stored at −70 °C until the time of analysis. The procedure for the fluorescence-based dNTP quantitative analysis was essentially as described previously with minor modifications (74). Specifically, both detection templates (DT) 1 and 2 for each dNTP were used, and the results were compared. Fluorescence signal was recorded every 5 min (1 cycle) for a total of 50 min (10 cycles) to monitor the kinetics of individual dNTP incorporation, and the fluorescence signal after a 40-min incubation (8 cycles) was used for calculation of the normalized fluorescence units. Standard curves using appropriate individual dNTPs were established for assay validation.

Spotting assay

Cells were grown to log phase at 30 °C, and 10-fold serial dilutions were spotted on the YPD plates with or without genotoxic chemicals and incubated at 30 °C for 48–72 h.

Statistical analysis

The results represent at least three independent experiments. Numerical results are presented as means ± S.D. Data were analyzed by using an InStat software package (Graphpad, San Diego). Statistical significance was evaluated by one-way analysis of variance, and $p < 0.05$ was considered significant.

Author contributions—P. B., I. V., and A. V. conceptualization; P. B., S. N., M. B., P. K., I. V., and A. V. data curation; P. B., S. N., M. B., and A. V. formal analysis; P. B. and A. V. supervision; P. B. and A. V. funding acquisition; P. B., S. N., M. B., and A. V. validation; P. B., S. N., M. B., P. K., A. S., J. Z., and A. V. investigation; P. B., S. N., M. B., P. K., A. S., and A. V. methodology; P. B., S. N., M. B., and A. V. writing-original draft; P. B. and A. V. project administration; P. B., I. V., and A. V. writing-review and editing; I. V. visualization.

Acknowledgments—We thank Drs. Barrientos, Chabes, Elledge, Kolodner, Stillman, Tyler, and Winston for strains and plasmids.

References

1. Kolodner, R. D., Putnam, C. D., and Myung, K. (2002) Maintenance of genome stability in *Saccharomyces cerevisiae*. *Science* **297,** 552–557 CrossRef Medline
2. Sancar, A., Lindsey-Boltz, L. A., Unsal-Kaçmaz, K., and Linn, S. (2004) Molecular mechanisms of mammalian DNA repair and the DNA damage checkpoints. *Annu. Rev. Biochem.* **73,** 39–85 CrossRef Medline
3. Ciccia, A., and Elledge, S. J. (2010) The DNA damage response: making it safe to play with knives. *Mol. Cell* **40,** 179–204 CrossRef Medline
4. Longhese, M. P., Foiani, M., Muzi-Falconi, M., Lucchini, G., and Plevani, P. (1998) DNA damage checkpoint in budding yeast. *EMBO J.* **17,** 5525–5528 CrossRef Medline
5. Putnam, C. D., and Kolodner, R. D. (2017) Pathways and mechanisms that prevent genome instability in *Saccharomyces cerevisiae*. *Genetics* **206,** 1187–1225 CrossRef Medline
6. Branzei, D., and Foiani, M. (2006) The Rad53 signal transduction pathway: replication fork stabilization, DNA repair, and adaptation. *Exp. Cell Res.* **312,** 2654–2659 CrossRef Medline
7. Putnam, C. D., Jaehnig, E. J., and Kolodner, R. D. (2009) Perspectives on the DNA damage and replication checkpoint responses in *Saccharomyces cerevisiae*. *DNA Repair* **8,** 974–982 CrossRef Medline
8. Polo, S. E., and Jackson, S. P. (2011) Dynamics of DNA damage response proteins at DNA breaks: a focus on protein modifications. *Genes Dev.* **25,** 409–433 CrossRef Medline
9. Zhou, C., Elia, A. E., Naylor, M. L., Dephoure, N., Ballif, B. A., Goel, G., Xu, Q., Ng, A., Chou, D. M., Xavier, R. J., Gygi, S. P., and Elledge, S. J. (2016) Profiling DNA damage-induced phosphorylation in budding yeast reveals diverse signaling networks. *Proc. Natl. Acad. Sci. U.S.A.* **113,** E3667–E3675 CrossRef Medline
10. O'Connor, M. J. (2015) Targeting the DNA damage response in cancer. *Mol. Cell* **60,** 547–560 CrossRef Medline
11. Bashkirov, V. I., Bashkirova, E. V., Haghnazari, E., and Heyer, W. D. (2003) Direct kinase-to-kinase signaling mediated by the FHA phosphoprotein recognition domain of the Dun1 DNA damage checkpoint kinase. *Mol. Cell. Biol.* **23,** 1441–1452 CrossRef Medline
12. Pellicioli, A., and Foiani, M. (2005) Signal transduction: how Rad53 kinase is activated. *Curr. Biol.* **15,** R769–771 CrossRef Medline
13. Zhou, Z., and Elledge, S. J. (1993) DUN1 encodes a protein kinase that controls the DNA damage response in yeast. *Cell* **75,** 1119–1127 CrossRef Medline
14. Chabes, A., Georgieva, B., Domkin, V., Zhao, X., Rothstein, R., and Thelander, L. (2003) Survival of DNA damage in yeast directly depends on increased dNTP levels allowed by relaxed feedback inhibition of ribonucleotide reductase. *Cell* **112,** 391–401 CrossRef Medline
15. Sabouri, N., Viberg, J., Goyal, D. K., Johansson, E., and Chabes, A. (2008) Evidence for lesion bypass by yeast replicative DNA polymerases during DNA damage. *Nucleic Acids Res.* **36,** 5660–5667 CrossRef Medline
16. Nordlund, P., and Reichard, P. (2006) Ribonucleotide reductases. *Annu. Rev. Biochem.* **75,** 681–706 CrossRef Medline
17. Hofer, A., Crona, M., Logan, D. T., and Sjöberg, B.-M. (2012) DNA building blocks: keeping control of manufacture. *Crit. Rev. Biochem. Mol. Biol.* **47,** 50–63 CrossRef Medline
18. Sanvisens, N., de Llanos, R., and Puig, S. (2013) Function and regulation of yeast ribonucleotide reductase: cell cycle, genotoxic stress, and iron bioavailability. *Biomed. J.* **36,** 51–58 CrossRef Medline
19. Mathews, C. K. (2015) Deoxyribonucleotide metabolism, mutagenesis and cancer. *Nat. Rev. Cancer* **15,** 528–539 CrossRef Medline
20. Huang, M., Zhou, Z., and Elledge, S. J. (1998) The DNA replication and damage checkpoint pathways induce transcription by inhibition of the Crt1 repressor. *Cell* **94,** 595–605 CrossRef Medline
21. Workman, C. T., Mak, H. C., McCuine, S., Tagne, J.-B., Agarwal, M., Ozier, O., Begley, T. J., Samson, L. D., and Ideker, T. (2006) A systems approach to mapping DNA damage response pathways. *Science* **312,** 1054–1059 CrossRef Medline
22. Tsaponina, O., Barsoum, E., Aström, S. U., and Chabes, A. (2011) Ixr1 is required for the expression of the ribonucleotide reductase Rnr1 and maintenance of dNTP pools. *PLoS Genet.* **7,** e1002061 CrossRef Medline
23. Travesa, A., Kuo, D., de Bruin, R. A., Kalashnikova, T. I., Guaderrama, M., Thai, K., Aslanian, A., Smolka, M. B., Yates, J. R., 3rd., Ideker, T., and Wittenberg, C. (2012) DNA replication stress differentially regulates G_1/S genes via Rad53-dependent inactivation of Nrm1. *EMBO J.* **31,** 1811–1822 CrossRef Medline
24. Bastos de Oliveira, F. M., Harris, M. R., Brazauskas, P., de Bruin, R. A., and Smolka, M. B. (2012) Linking DNA replication checkpoint to MBF cell-cycle transcription reveals a distinct class of G_1/S genes. *EMBO J.* **31,** 1798–1810 CrossRef Medline

25. Yao, R., Zhang, Z., An, X., Bucci, B., Perlstein, D. L., Stubbe, J., and Huang, M. (2003) Subcellular localization of yeast ribonucleotide reductase regulated by the DNA replication and damage checkpoint pathways. *Proc. Natl. Acad. Sci. U.S.A.* **100,** 6628–6633 CrossRef Medline
26. Lee, Y. D., and Elledge, S. J. (2006) Control of ribonucleotide reductase localization through an anchoring mechanism involving Wtm1. *Genes Dev.* **20,** 334–344 CrossRef Medline
27. Zhang, Z., An, X., Yang, K., Perlstein, D. L., Hicks, L., Kelleher, N., Stubbe, J., and Huang, M. (2006) Nuclear localization of the *Saccharomyces cerevisiae* ribonucleotide reductase small subunit requires a karyopherin and a WD40 repeat protein. *Proc. Natl. Acad. Sci. U.S.A.* **103,** 1422–1427 CrossRef Medline
28. Lee, Y. D., Wang, J., Stubbe, J., and Elledge, S. J. (2008) Dif1 is a DNA-damage-regulated facilitator of nuclear import for ribonucleotide reductase. *Mol. Cell* **32,** 70–80 CrossRef Medline
29. Wu, X., and Huang, M. (2008) Dif1 controls subcellular localization of ribonucleotide reductase by mediating nuclear import of the R2 subunit. *Mol. Cell. Biol.* **28,** 7156–7167 CrossRef Medline
30. Sanvisens, N., Romero, A. M., Zhang, C., Wu, X., An, X., Huang, M., and Puig, S. (2016) Yeast Dun1 kinase regulates ribonucleotide reductase small subunit localization in response to iron deficiency. *J. Biol. Chem.* **291,** 9807–9817 CrossRef Medline
31. Zhao, X., Muller, E. G., and Rothstein, R. (1998) A suppressor of two essential checkpoint genes identifies a novel protein that negatively affects dNTP pools. *Mol. Cell* **2,** 329–340 CrossRef Medline
32. Zhao, X., Chabes, A., Domkin, V., Thelander, L., and Rothstein, R. (2001) The ribonucleotide reductase inhibitor Sml1 is a new target of the Mec1/Rad53 kinase cascade during growth and in response to DNA damage. *EMBO J.* **20,** 3544–3553 CrossRef Medline
33. Zhao, X., and Rothstein, R. (2002) The Dun1 checkpoint kinase phosphorylates and regulates the ribonucleotide reductase inhibitor Sml1. *Proc. Natl. Acad. Sci. U.S.A.* **99,** 3746–3751 CrossRef Medline
34. Andreson, B. L., Gupta, A., Georgieva, B. P., and Rothstein, R. (2010) The ribonucleotide reductase inhibitor, Sml1, is sequentially phosphorylated, ubiquitylated and degraded in response to DNA damage. *Nucleic Acids Res.* **38,** 6490–6501 CrossRef Medline
35. Eriksson, P. R., Ganguli, D., Nagarajavel, V., and Clark, D. J. (2012) Regulation of histone gene expression in budding yeast. *Genetics* **191,** 7–20 CrossRef Medline
36. Kurat, C. F., Recht, J., Radovani, E., Durbic, T., Andrews, B., and Fillingham, J. (2014) Regulation of histone gene transcription in yeast. *Cell. Mol. Life Sci.* **71,** 599–613 CrossRef Medline
37. Gasch, A. P., Huang, M., Metzner, S., Botstein, D., Elledge, S. J., and Brown, P. O. (2001) Genomic expression responses to DNA-damaging agents and the regulatory role of the yeast ATR homolog Mec1p. *Mol. Biol. Cell* **12,** 2987–3003 CrossRef Medline
38. Su, C., Gao, G., Schneider, S., Helt, C., Weiss, C., O'Reilly, M. A., Bohmann, D., and Zhao, J. (2004) DNA damage induces downregulation of histone gene expression through the G_1 checkpoint pathway. *EMBO J.* **23,** 1133–1143 CrossRef Medline
39. Libuda, D. E., and Winston, F. (2010) Alterations in DNA replication and histone levels promote histone gene amplification in *Saccharomyces cerevisiae*. *Genetics* **184,** 985–997 CrossRef Medline
40. Galdieri, L., Zhang, T., Rogerson, D., and Vancura, A. (2016) Reduced histone expression or a defect in chromatin assembly induces respiration. *Mol. Cell. Biol.* **36,** 1064–1077 CrossRef Medline
41. Huang, M. E., and Kolodner, R. D. (2005) A biological network in *Saccharomyces cerevisiae* prevents the deleterious effects of endogenous oxidative DNA damage. *Mol. Cell* **17,** 709–720 CrossRef Medline
42. Ragu, S., Faye, G., Iraqui, I., Masurel-Heneman, A., Kolodner, R. D., and Huang, M. (2007) Oxygen metabolism and reactive oxygen species cause chromosomal rearrangements and cell death. *Proc. Natl. Acad. Sci. U.S.A.* **104,** 9747–9752 CrossRef Medline
43. Simpson-Lavy, K. J., Bronstein, A., Kupiec, M., and Johnston, M. (2015) Cross-talk between carbon metabolism and the DNA damage response in *S. cerevisiae*. *Cell Rep.* **12,** 1865–1875 CrossRef Medline
44. Bolzán, A. D., and Bianchi, M. S. (2018) DNA and chromosome damage induced by bleomycin in mammalian cells: an update. *Mutat. Res.* **775,** 51–62 CrossRef Medline
45. Friedberg, E. C. (1995) Out of the shadows and into the light: the emergence of DNA repair. *Trends Biochem. Sci.* **20,** 381 CrossRef Medline
46. Zhang, T., Bu, P., Zeng, J., and Vancura, A. (2017) Increased heme synthesis in yeast induces a metabolic switch from fermentation to respiration even under conditions of glucose repression. *J. Biol. Chem.* **292,** 16942–16954 CrossRef Medline
47. Mortensen, U. H., Lisby, M., and Rothstein, R. (2009) Rad52. *Curr. Biol.* **19,** R676–R677 CrossRef Medline
48. Taylor, S. D., Zhang, H., Eaton, J. S., Rodeheffer, M. S., Lebedeva, M. A., O'rourke, T. W., Siede, W., and Shadel, G. S. (2005) The conserved Mec1/rRd53 nuclear checkpoint pathway regulates mitochondrial DNA copy number in *Saccharomyces cerevisiae*. *Mol. Biol. Cell* **16,** 3010–3018 CrossRef Medline
49. Rando, O. J., and Winston, F. (2012) Chromatin and transcription in yeast. *Genetics* **190,** 351–387 CrossRef Medline
50. Tsankov, A. M., Thompson, D. A., Socha, A., Regev, A., and Rando, O. J. (2010) The role of nucleosomes positioning in the evolution of gene regulation. *PLoS Biol.* **8,** e1000414 CrossRef Medline
51. Gunjan, A., and Verreault, A. (2003) A Rad53 kinase-dependent surveillance mechanism that regulates histone protein levels in *S. cerevisiae*. *Cell* **115,** 537–549 CrossRef Medline
52. Singh, R. K., Kabbaj, M. H., Paik, J., and Gunjan, A. (2009) Histone levels are regulated by phosphorylation and ubiquitylation-dependent proteolysis. *Nat. Cell Biol.* **11,** 925–933 CrossRef Medline
53. Osley, M. A., and Lycan, D. (1987) Trans-acting regulatory mutations that alter transcription of *Saccharomyces cerevisiae* histone genes. *Mol. Cell. Biol.* **7,** 4204–4210 CrossRef Medline
54. Xu, H., Kim, U. J., Schuster, T., and Grunstein, M. (1992) Identification of a new set of cell cycle-regulatory genes that regulate S-phase transcription of histone genes in *Saccharomyces cerevisiae*. *Mol. Cell. Biol.* **12,** 5249–5259 CrossRef Medline
55. Misko, T. A., Wijerathna, S. R., Radivoyevitch, T., Berdis, A. J., Ahmad, M. F., Harris, M. E., and Dealwis, C. G. (2016) Inhibition of yeast ribonucleotide reductase by Sml1 depends on the allosteric state of the enzyme. *FEBS Lett.* **590,** 1704–1712 CrossRef Medline
56. Ocampo, A., Liu, J., Schroeder, E. A., Shadel, G. S., and Barrientos, A. (2012) Mitochondrial respiratory tresholds regulate yeast chronological life span and its extension by caloric restriction. *Cell Metab.* **16,** 55–67 CrossRef Medline
57. Chabes, A., and Stillman, B. (2007) Constitutively high dNTP concentration inhibits cell cycle progression and the DNA damage checkpoint in yeast *Saccharomyces cerevisiae*. *Proc. Natl. Acad. Sci. U.S.A.* **104,** 1183–1188 CrossRef Medline
58. Sidorova, J. M., and Breeden, L. L. (1997) Rad53-dependent phosphorylation of Swi6 and down-regulation of CLN1 and CLN2 transcription occur in response to DNA damage in *Saccharomyces cerevisiae*. *Genes Dev.* **11,** 3032–3045 CrossRef Medline
59. Sidorova, J. M., and Breeden, L. L. (2003) Rad53 checkpoint kinase phosphorylation site preference identified in the Swi6 protein of *Saccharomyces cerevisiae*. *Mol. Cell. Biol.* **23,** 3405–3416 CrossRef Medline
60. Jaehnig, E. J., Kuo, D., Hombauer, H., Ideker, T. G., and Kolodner, R. D. (2013) Checkpoint kinases regulate a global network of transcription factors in response to DNA damage. *Cell Rep.* **4,** 174–188 CrossRef Medline
61. Hess, D., and Winston, F. (2005) Evidence that Spt10 and Spt21 of *Saccharomyces cerevisiae* play distinct roles *in vivo* and functionally interact with MCB-binding factor, SCB-binding factor and Snf1. *Genetics* **170,** 87–94 CrossRef Medline
62. Yao, N. Y., Schroeder, J. W., Yurieva, O., Simmons, L. A., and O'Donnell, M. E. (2013) Cost of rNTP/dNTP pool imbalance at the replication fork. *Proc. Natl. Acad. Sci. U.S.A.* **110,** 12942–12947 CrossRef Medline
63. Watt, D. L., Buckland, R. J., Lujan, S. A., Kunkel, T. A., and Chabes, A. (2016) Genome-wide analysis of the specificity and mechanisms of replication infidelity driven by imbalanced dNTP pools. *Nucleic Acids Res.* **44,** 1669–1680 CrossRef Medline

64. Schmidt, T. T., Reyes, G., Gries, K., Ceylan, C. Ü., Sharma, S., Meurer, M., Knop, M., Chabes, A., and Hombauer, H. (2017) Alterations in cellular metabolism triggered by URA7 or GLN3 inactivation cause imbalanced dNTP pools and increased mutagenesis. *Proc. Natl. Acad. Sci. U.S.A.* **114,** E4442–E4451 CrossRef Medline
65. Finkel, T. (2003) Oxidant signals and oxidative stress. *Curr. Opin. Cell Biol.* **15,** 247–254 CrossRef Medline
66. Balaban, R. S., Nemoto, S., and Finkel, T. (2005) Mitochondria, oxidants, and aging. *Cell* **120,** 483–495 CrossRef Medline
67. Barros, M. H., bandy, B., Tahara, E. B., and Kowaltowski, A. J. (2004) Higher respiratory activity decreases mitochondrial reactive oxygen release and increases life span in *Saccharomyces cerevisiae*. *J. Biol. Chem.* **279,** 49883–49888 CrossRef Medline
68. Brace, L. E., Vose, S. C., Stanya, K., Gathungu, R. M., Marur, V. R., Longchamp, A., Trevino-Villarreal, H., Mejia, P., Vargas, D., Inouye, K., Bronson, R. T., Lee, C. H., Neilan, E., Kristal, B. S., and Mitchell, J. R. (2016) Increased oxidative phosphorylation in response to acute and chronic DNA damage. *NPJ Aging Mech. Dis.* **2,** 16022 CrossRef Medline
69. Kitanovic, A., Walther, T., Loret, M. O., Holzwarth, J., Kitanovic, I., Bonowski, F., Van Bui, N., Francois, J. M., and Wölfl, S. (2009) Metabolic response to MMS-mediated DNA damage in *Saccharomyces cerevisiae* is dependent on the glucose concentration in the medium. *FEMS Yeast Res.* **9,** 535–551 CrossRef Medline
70. Yu, Y., Eriksson, P., and Stillman, D. J. (2000) Architectural transcription factors and the SAGA complex function in parallel pathways to activate transcription. *Mol. Cell. Biol.* **20,** 2350–2357 CrossRef Medline
71. Sherman, F. (1991) Getting started with yeast. *Methods Enzymol.* **194,** 3–21 CrossRef Medline
72. Stuart, D., and Wittenberg, C. (1995) CLN3, not positive feedback, determines the timing of *CLN2* transcription in cycling cells. *Genes Dev.* **9,** 2780–2794 CrossRef Medline
73. Galdieri, L., and Vancura, A. (2012) Acetyl-CoA carboxylase regulates global histone acetylation. *J. Biol. Chem.* **287,** 23865–23876 CrossRef Medline
74. Wilson, P. M., Labonte, M. J., Russell, J., Louie, S., Ghobrial, A. A., and Ladner, R. D. (2011) A novel fluorescence-based assay for the rapid detection and quantification of cellular deoxyribonucleoside triphosphates. *Nucleic Acids Res.* **39,** e112 CrossRef Medline